Master Thesis

# Mitigation of Cancellation Problem & Introduction of GKW $f$ version

Manuel Lippert

Submission date: September 10, 2024

**Physics Department at the University of Bayreuth**

Supervisors:
Prof. Arthur G. Peeters
Dr. Florian Rath

★ 07.07.2020 - † 09.08.2024

This thesis is dedicated to my cat **Leo**
who is part of our family since July 2020.
He is the kindest cat I ever own and very playful.
I will miss our walks together and you accompany in my life.

I love you.

Manuel Lippert

# Declaration

The author states that every information, regarding this thesis can be found under the GitHub Repository with the link `https://github.com/ManeLippert/Masterthesis-Parallel-Electric-Field`.

# Contents

CHAPTER

# 1

# Motivation

Plasma can be described in various theoretical models. The main two models are the Magnetohydrodynamics and the kinetic model. The key differences will be briefly explained

- **Magnetohydrodynamics:**
  In Magnetohydrodynamics the plasma will be described as an electric conductiv fluid which carries current. Here, the electrons and ions are two mixed fluids expressed in the two-fluid theory. In both description macroscopic quantities will be used, i.e. density, velocity of the fluid and temperature.
- **Kinetic Model:**
  In the kinetic model the plasma will be described in the sixdimensional phase space through the Vlasov equation. In combination with the Maxwell's equations is it possible to discribe the dynamics of the plasma as the Vlasov-Maxwell system.

In this section the kinetic model will be covered in greater detail for that the following scheme will be used:

1. The Lagrangian $L$ for a particle in a magnetic field will reformulate in the fundamental one-form $\gamma$ according to

$$\int \mathrm{d}t\ L = \int \gamma\ . \tag{1.1}$$

   From this point on the fundamental one-form and Lagrangian referres to the quantity $\gamma$, which will only be used in this thesis. Then, the Lagrangian $\gamma$ will be transformed in guiding center phase space and separated in its equilibrium and perturbated part. Through the Lietransformation the Lagrangian gets transformed intop the gyrtocenter phase space by eliminating the gyro phase.
2. The Lagrangian gets plugged in to the Euler-Lagrangian equation, which results in the equations of motions. From the equations of motion the Vlasov equation can be derived.
3. The Vlasov equation solves for the density distribution function $f$, which will be used to express the particle density $n$ and current $\mathbf{j}$ with the moments of the distrubution function.
4. Particle density $n$ and current $\mathbf{j}$ will be plugged into the Maxwell's equations and the field equations of the potentials will be derived.

This part of the thesis is based on the Disseratation of Tilman Dannert[6] and the derivation document provided from the **GKW** group[20]. For the introduction of the inductive electric field the Disseratation of Paul Charles Crandall[4] will be used to formulate the electromagnetic gyrokinetic model for **GKW** .

CHAPTER

# 2

# Plasma Physics Basics

## 2.1 Charged Particle Motion in Magnetic and Electric Field

In magnetic confinement devices like the tokamak reactor, the charged particles experience forces caused by magnetic and electric fields which results in distinct motion under the associated force. Charged particles can be separated in species, e.g. electrons and ions, which will be later on not displayed in the governing equation. Throughout this thesis the charge $q$, the mass $m$ or the temperature $T$ indicate the quantities of a specific species, i.e., electrons or ions.

### 2.1.1 Particle Motion perpendicular to the Magnetic Field

Due to the Lorentz force, particles with a velocity component perpendicular to the homogenous magnetic field $v_\perp$ undergo a circular motion in the plane perpendicular to the magnetic field [Fig. 2.1(a)]. This type of motion has circular frequency, which is often referred to as *cyclotron frequency* and is defined as

$$\omega_\mathrm{c} = \frac{|q|B}{m} \ , \tag{2.1}$$

where $m$ and $q$ are the mass and the charge of the particle and $B$ the strength of the magnetic field. The radius, the so called *Larmor radius*, of this motion is given by

$$\rho = \frac{mv_\perp}{|q|B} \tag{2.2}$$

with the center often being referred to as *gyrocenter*. Note that since the Lorentz force depends on the species charge of the particle, the circulation direction is the opposite between electron in ions.

Due to Coulomb collisions the plasma gets thermalized. Together with the Maxwell-Boltzmann distribution the typical thermal velocity is

$$v_\mathrm{th} = \sqrt{\frac{2T}{m}} \ , \tag{2.3}$$

where $T$ represents the species temperature. Based on the thermal velocity $v_\mathrm{th}$ the *thermal Larmor radius* gets introduced as[22]

$$\rho_\mathrm{th} = \frac{mv_\mathrm{th}}{|q|B} \ . \tag{2.4}$$

### 2.1.2 Particle Motion parallel to the Magnetic Field

In absence of forces in the direction parallel to the magnetic field the particles can move freely in parallel direction to the homogenous magnetic field. The velocity of this motion is of order of the thermal velocity $v_{\mathrm{th}}$ and is dominated by electrons due to their lighter mass compared to ions ($v_{\mathrm{th,e}}/v_{\mathrm{th,i}} = 60$).

When an electric field with a component parallel to the magnetic field $E_{\parallel}$ influences the plasma the charged particles are accelerated by the electric force

$$F_{\parallel,E} = qE_{\parallel} \ . \tag{2.5}$$

The parallel motion follows then from the equation of motion. Here the direction of the motion also depends on the species type [Fig. 2.1(b)].

Since magnetic fields are not always homogenous, an inhomogeneous magnetic field with its gradient $\nabla B$ containing a component parallel to the magnetic field which is given by

$$\nabla_{\parallel} B = \frac{\mathbf{B}}{B} \cdot \nabla B \tag{2.6}$$

causes the force

$$F_{\parallel,\nabla_{\parallel}B} = -\frac{mv_{\perp}^2}{2B}\nabla_{\parallel} B = -\mu \nabla_{\parallel} B \ ; \qquad \mu = \frac{mv_{\perp}^2}{2B} \tag{2.7}$$

with *magnetic moment* $\mu$. The magnetic moment $\mu$ is an adabatic invariant (constant of motion) if the variation of the magnetic field over time is smaller than the inverse of the cyclotron frequency $\omega_{\mathrm{c}}^{-1}$ and the spatial variation is larger the Larmor radius $\rho_{\mathrm{L}}$. The resulting force has its application in the mirror effect where a charged particle gets reflected due to this force [Fig. 2.1(c)].[22]

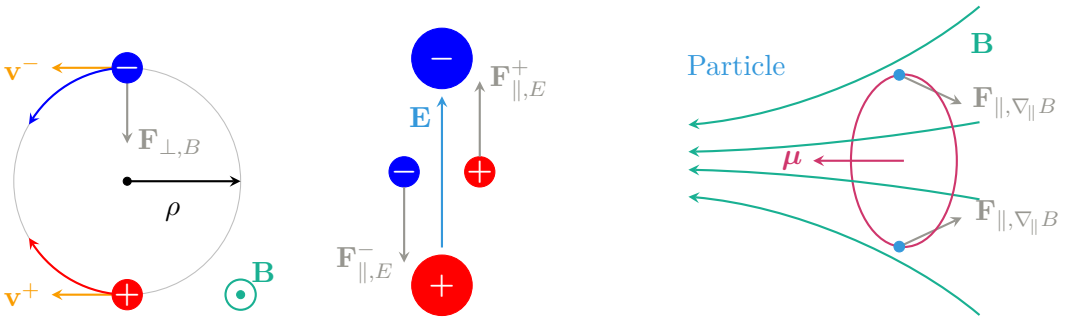


**(a)** **(b)** **(c)**

Figure 2.1: Forces acting on a charged particle:

- **(a)** Lorentz force $\mathbf{F}_{\perp,B}$ perpendicular to velocity $\mathbf{v}^{\pm}$ and magnetic field $\mathbf{B}$ which causes, circular motion with different directions for electron and ions, Lamor radius $\rho_{\mathrm{L}}$ and cyclotron frequency $\omega_{\mathrm{c}}$,
- **(b)** Electric force $\mathbf{F}^{\pm}_{\parallel,E}$ with electric field $\mathbf{E}$,
- **(c)** Mirror effect with force $\mathbf{F}_{\parallel,\nabla_{\parallel}B}$ and magnetic moment $\mu$ caused by an inhomogeneous magnetic field $\mathbf{B}$.

### 2.1.3 Drifts in the Gyrocenter

In the presence of a magnetic field (homogenous, inhomogeneous or perturbed) and electric fields the gyrocenter undergoes slow (compared to the thermal velocity $v_{\mathrm{th}}$) drift motions perpendicular to the magnetic field. There are several examples for this drift motion. According to this thesis topic only the main three drift types will be covered in the following.

1. **E × B Drift:**
   If an electric field **E** with a perpendicular component together with the magnetic field **B** (both fields are homogenous) is present the acting Coulomb force and Lorentz force results into a drift of the gyrocenter with

$$\mathbf{v}_E = \frac{\mathbf{E} \times \mathbf{B}}{B^2} \tag{2.8}$$

   which is called the E × B drift. Since both acting forces direction depends on the species type the direction of the E × B drift is for every species the same [Fig. 2.2(a)].

2. **$\nabla B$ Drift:**
   Inhomogeneous magnetic field causes a gradient $\nabla B$ of the magnetic field. Because of that gradient the gyrocenter undergoes a $\nabla B$ drift defined by

$$\mathbf{v}_{\nabla B} = \frac{m v_\perp^2}{2q} \frac{\mathbf{B} \times \nabla B}{B^3} \ . \tag{2.9}$$

   The gradient of the magnetic field $\nabla B$ varies thereby on scales larger compared to the Larmor radius. The direction of the $\nabla B$ drift depends on the species type [Fig. 2.2(b)].

3. **Curvature Drift:**
   Due to centrifugal force acting on the particle in a curved magnetic field the gyrocenter experiences a curvature drift according to

$$\mathbf{v}_C = \frac{m v_\parallel^2}{q} \frac{\mathbf{B} \times \mathbf{C}}{B^2} = \frac{m v_\parallel^2}{q} \frac{\mathbf{B} \times \nabla B}{B^3} \ ; \qquad \mathbf{C} = -(\mathbf{b} \cdot \nabla)\mathbf{b} = \frac{\nabla B}{B} \ , \tag{2.10}$$

   where **b** is the unit vector along the magnetic field. To obtain the result for the curvature **C** in Eq. (2.10) the plasma pressure has to be small compared to the magnetic field strength $B$. In the form of Eq. (2.10) $\nabla B$ and curvature drift can be treated similarly.[22]

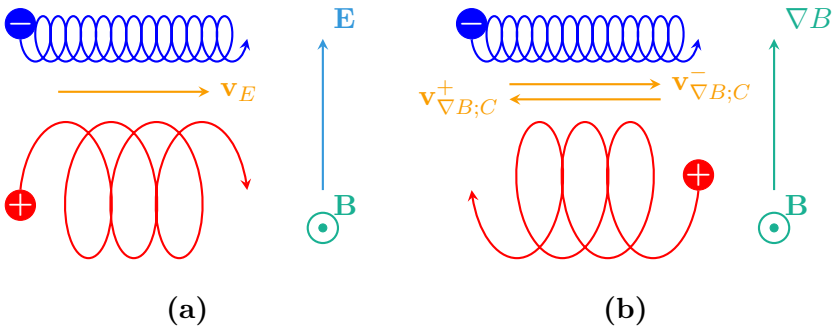


Figure 2.2: Dirft motion in gyrocenter:

**(a)** E × B Drift with drift velocity $\mathbf{v}_E$, electric field **E** and magnetic field **B**,

**(b)** $\nabla B$ Drift/Curvature Drift with drift velocity $\mathbf{v}^{\pm}_{\nabla B;\kappa}$, magnetic field **B** and gradient of the magnetic field $\nabla B$.

## 2.2 Magnetic Confinement and Plasma Rotation

In tokamak devices strong magnetic fields confine the hot plasma. As mentioned in Chapter 2.1 a magnetic field forces a perpendicular particle motion and a motion which contains the gyro motion and slow perpendicular gyro center drifts. Because of the much smaller size of the Larmor radius compared to the device size $R$ the particle and energy losses are caused by the gyro center drift. To avoid additional loss of particles because of the parallel motion the field lines of the magnetic field in the tokamak devices is shaped like a torus. This type of geometry has nested surfaces with constant magnetic flux, so-called *flux surfaces*, and magnetic field lines which lie on these surfaces. To maintain stability the magnetic field has a toroidal and a poloidal component. According to the force balance the magnetic field is equivalent to the plasma pressure which means on flux-surfaces the plasma pressure is constant.[19,22] The toroidal component is produced by external coils whereas the poloidal component is provided by the toroidal plasma current. Together the components result in a magnetic field which follows helical trajectories [Fig 2.3]. To characterize the quality of confinement the so-called *plasma beta* is used and is given as

$$\beta = \frac{nT}{B^2/2\mu_0} \ , \tag{2.11}$$

with $n$ the plasma density, $T$ as temperature, $\mu_0$ the permeability in vacuum and the magnetic field strength $B$. Respectively, the plasma beta compares the thermal plasma pressure $nT$ to the ambient magnetic field pressure $B^2/2\mu_0$. For fusion devices the plasma beta has to be a bit smaller than 1 ($\beta < 1$) for optimal confinement. In a tokamak reactor the plasma beta has a typical order of a few percent.[22]

The rotation of the plasma can be described in a co-rotating frame of reference, which is rigidly rotating with the velocity $\mathbf{u}_0$ and will be used later on in the derivation of the gyrokinetic equations in Chapter 3.2. It assumend that the poloidal component of the plasma rotation is much smaller compared to the toridial component and will be neglected. With this assumption in mind the reference frame is chosen to move in the toridial direction exclusivly and its velocity $\mathbf{u}_0$ can be expressed as

$$\mathbf{u}_0 = \mathbf{\Omega} \times \mathbf{x} = R^2 \Omega \nabla \varphi \ , \tag{2.12}$$

where $\mathbf{\Omega}$ is the constant angular frequency, $\varphi$ is the toroidal angle and $R\nabla\varphi$ is the unit vector in the toroidal direction.

Since the rotation of the plasma in the labortory frame is not a rigid body rotation, it will be characterized by the radial profile of the angular velocity $\hat{\Omega}(\psi)$. Then the angular frequency of the rotating frame $\Omega$ is chosen to match the plasma rotation on a certain point, i.e. $\Omega = \hat{\Omega}(\psi_r)$. The plasma rotation in the co-rotating frame of reference will be denoted as

$$\omega_\varphi(\psi) = \hat{\Omega}(\psi) - \Omega. \tag{2.13}$$

with the rotation speed along the magnetic field line

$$u_\parallel = \frac{RB_\mathrm{t}}{B}\omega_\varphi(\psi)\ , \tag{2.14}$$

where $B_\mathrm{t}$ is the toridial component of the magnetic field.[16]

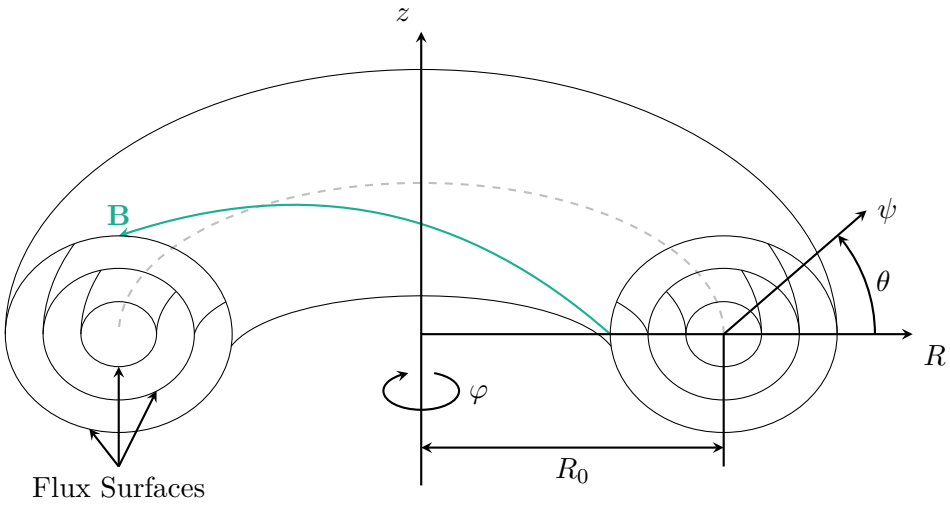


Figure 2.3: Toroidal flux surfaces in tokamak plasma with helical magnetic field (green line) in torus coordinates ($\psi$ (radial), $\varphi$ (toroidal), $\theta$ (poloidal)) or cylindrical coordinates ($z$, $R$, $-\varphi$).[1]

CHAPTER

# Derivation of Gyrokinetic Equation

3

## 3.1 Gyrokinetic Ordering

In the derivation of the gyrokinetic theory the aim is to decouple the effect of small-scale, small amplitude fluctuations of the plasma in the Langrangian. For this it is chosen to take the properties of fluctuations as small parameter, which will result in the ordering assumptions applied in gyrokinetic theory. This section is based on Ref. 2 and 10.

- **Low Frequency**:
  The characteristic fluctuation frequency is small compared to the cyclotron frequency
  $$\Rightarrow \frac{\omega}{\omega_\mathrm{c}} \ll 1 \ .$$
- **Anisotropy**:
  The length scales of the turbulence are associated with the wave vector $\mathbf{k}$ which can be seperated into a perpendicular component $k_\perp = |\mathbf{k} \times \mathbf{b}|$ and a parallel component $k_\parallel = |\mathbf{k} \cdot \mathbf{b}|$ where $\mathbf{b}$ is parallel to the poloidal component of the magnetic field. The perpendicular correlation length of the turbulance has a length scale of around $10 - 100$ gyroradii while the parallel length scales can be of the order of meters, which can be expressed in wavenaumber as
  $$\Rightarrow \frac{k_\parallel}{k_\perp} \ll 1 \ .$$
- **Strong Magnetization**:
  The Larmor radius $\rho$ is small compared to the gradient length scales for
  - Background Density: $L_n = n_0 \left(\frac{\mathrm{d}n_0}{\mathrm{d}x}\right)^{-1}$
  - Background Temperature: $L_T = T_0 \left(\frac{\mathrm{d}T_0}{\mathrm{d}x}\right)^{-1}$
  - Background Magnetic Field: $L_B = B_0 \left(\frac{\mathrm{d}B_0}{\mathrm{d}x}\right)^{-1}$

  $$\Rightarrow \frac{\rho}{L_n} \sim \frac{\rho}{L_T} \sim \frac{\rho}{L_B} \ll 1 \ .$$
- **Small Fluctuations**:
  The fluctuating part of the gyrocenter distribution function $F_1$ is assumend to be small compared to the background distribution function $F_0$
  $$\Rightarrow \frac{F_1}{F_0} \ll 1 \ .$$
  Furthermore, the fluctuations of the vector potential $\mathbf{A}_1$ and scalar potentials $\Phi_1$ are small compared to there background part
  $$\Rightarrow \frac{\mathbf{A}_1}{\mathbf{A}_0} \sim \frac{\Phi_1}{\Phi_0} \ll 1 \ .$$

Taken together these assumptions leads to the gyrokinetic ordering

$$\frac{\omega}{\omega_{\mathrm{c}}} \sim \frac{k_{\parallel}}{k_{\perp}} \sim \frac{\rho}{L_n} \sim \frac{\rho}{L_T} \sim \frac{\rho}{L_B} \sim \frac{F_1}{F_0} \sim \frac{\mathbf{A}_1}{\mathbf{A}_0} \sim \frac{\Phi_1}{\Phi_0} \sim \epsilon_\delta \ , \tag{3.1}$$

where $\epsilon_\delta$ is a small parameter. For the derivation of the gyrokinetic equations of **GKW** all derived equations are evaluated up to the first order of the ratio of the reference thermal Larmor radius $\rho_{\mathrm{th,ref}}$ and the equilibrium magnetic length scale $L_B$ as small parameter and is defined as

$$\rho_\star = \frac{\rho_{\mathrm{th,ref}}}{L_B} = \frac{m_{\mathrm{ref}} v_{\mathrm{th,ref}}}{e B_{\mathrm{ref}}} \sim \epsilon_\delta \ . \tag{3.2}$$

## 3.2 Gyrokinetic Lagrangian (Fundamental One-Form)

### 3.2.1 Lagrangian in Patricle Phase Space

The Lagrangian of a particle $\gamma$ with mass $m$ and charge number $Z$ in the electro magnetic field will be described through the particle position $\mathbf{x}$ and the velocity $\mathbf{v}$ as coordinates $\{\mathbf{x}, \mathbf{v}\}$ and can be written as

$$\gamma = \gamma_\nu \mathrm{d}z^\nu = \underbrace{(m\mathbf{v} + Ze\mathbf{A}(\mathbf{x}))}_{\text{Sympletic Part}} \cdot \mathrm{d}\mathbf{x} - \underbrace{\left(\frac{1}{2}mv^2 + Ze\Phi(\mathbf{x})\right)}_{\text{Hamiltonian } H(\mathbf{x},\mathbf{v})} \mathrm{d}t \ , \tag{3.3}$$

where $\mathbf{A}$ and $\Phi$ are the vector and scalar potential, $\nu$ indexes the six coordinates, and Einstein notation is applied. This form is also known as fundamental one-form.

The defined Lagrangian $\gamma$ will then be transformed in the rotating frame of reference [Ch. 2.2], which can be achieved the following Lorentz transformation

$$\mathbf{v} \to \mathbf{v} + \mathbf{u}_0 \qquad \mathbf{E} \to \mathbf{E} + \mathbf{u}_0 \times \mathbf{B} \qquad \Phi \to \Phi + \mathbf{A} \cdot \mathbf{u}_0 \ . \tag{3.4}$$

After performing the transformation outlined in Ref. 16 the Lagrangian $\gamma$ becomes

$$\gamma = (m\mathbf{v} + m\mathbf{u}_0 + Ze\mathbf{A}(\mathbf{x})) \cdot \mathrm{d}\mathbf{x} - \left(\frac{1}{2}mv^2 - \frac{1}{2}mu_0^2 + Ze\Phi(\mathbf{x})\right) \mathrm{d}t \ . \tag{3.5}$$

In the next step small scale perturbations of the electromagnetic field gets introduced as following

$$\Phi = \Phi_0 + \Phi_1 \qquad \mathbf{A} = \mathbf{A}_0 + \mathbf{A}_1 \ . \tag{3.6}$$

Here, it is assumend that the equilibrium electric field is zero in a stationary plasma, but it will be kept in case for finite plasma rotation. According to the gyrokinetic ordering [Ch. 3.1] the perturbations are in the first order of $\rho_\star$. Taking everything into account the Lagrangian in the particle phase space with perturbations can be written as

$$\begin{aligned} \gamma &= \gamma_0 + \gamma_1 \\ \gamma_0 &= (m\mathbf{v} + m\mathbf{u}_0 + Ze\mathbf{A}_0(\mathbf{x})) \cdot \mathrm{d}\mathbf{x} - \left(\frac{1}{2}mv^2 - \frac{1}{2}mu_0^2 + Ze\Phi_0(\mathbf{x})\right) \mathrm{d}t \\ \gamma_1 &= Ze\mathbf{A}_1(\mathbf{x}) \cdot \mathrm{d}\mathbf{x} - Ze\Phi_1(\mathbf{x}) \, \mathrm{d}t \ . \end{aligned} \tag{3.7}$$

### 3.2.2 Lagrangian in Guiding Center Phase Space

For the description of charged particle behaviour in the tokamak device the *guiding center coordinates* are used [Fig. 3.1]. This set of coordinates are defined as the following

$$\begin{aligned} \mathbf{X}(\mathbf{x},\mathbf{v}) &= \mathbf{x} - \mathbf{r} & v_\parallel &= \mathbf{v}\cdot\mathbf{b}(\mathbf{x}) \\ \mu(\mathbf{x},\mathbf{v}) &= \frac{m v_\perp^2(\mathbf{x})}{2B(\mathbf{x})} & \theta(\mathbf{x},\mathbf{v}) &= \arccos\left(\frac{1}{v_\perp}\left(\mathbf{b}(\mathbf{x})\times\mathbf{v}\right)\cdot\hat{\mathbf{e}}_1\right) \ , \end{aligned} \tag{3.8}$$

where the guiding center follows the magnetic field with the parallel velocity $v_\parallel$. The gyromotion is described together with the magnetic moment $\mu$, the guiding center $\mathbf{X}$ and the gyro phase $\theta$ which gives a parameter set of six quantities $\{\mathbf{X}, v_\parallel, \mu, \theta\}$. Vector $\mathbf{b}(\mathbf{x})$ is the unit vector in the direction of the equilibrium magnetic field and $\mathbf{r} = \rho(\mathbf{x},\mathbf{v})\mathbf{a}(\mathbf{x},\mathbf{v})$ is the vector pointing from the guiding center to the particles postion, which is defined by the unit vector $\mathbf{a}(\mathbf{x},\mathbf{v})$ and its length is the Lamor radius $\rho(\mathbf{x},\mathbf{v})$. The unit vector $\mathbf{a}(\mathbf{x},\mathbf{v})$ can be expressed in a local orthonormal basis as the function of the gyroangle $\theta$

$$\mathbf{a}(\theta) = \hat{\mathbf{e}}_1\cos\theta + \hat{\mathbf{e}}_2\sin\theta \ . \tag{3.9}$$

The vectors $\mathbf{b}$, $\hat{\mathbf{e}}_1$ and $\hat{\mathbf{e}}_2$ form a local Cartesian coordinate system at the guiding center position.

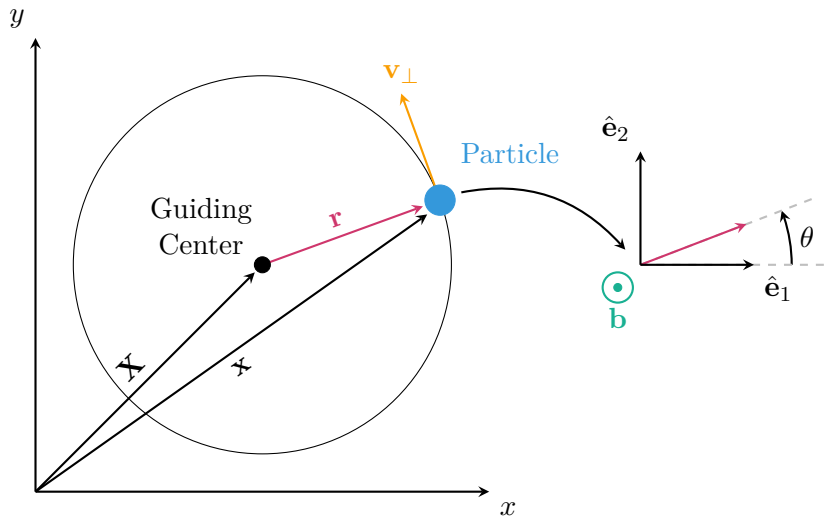


Figure 3.1: Sketch of guiding center coordinates where the charged particle performs a circular motion around the guiding center.[8]

To transform the fundamental one-from into the guiding center coordinates the following relation will be used

$$\Gamma_\eta = \gamma_\nu \frac{\mathrm{d}z^\nu}{\mathrm{d}Z^\eta} \ , \tag{3.10}$$

where $\Gamma_\eta$ is a component of the guiding center fundamental one-form. To calculate the new coordinates the transformation [Eq. (3.8)] have to be inverted to provide the old coordinates as function of the new one $z(Z)$. Here, the direct transformation is clearly uniquely determined if the magnetic field is known at the particle postion. However, the inverse transformation is not uniquely due to the dependence of the Larmor radius $\rho$ on magnetic field at the particle position $\mathbf{x}$. Taylor expansion of the Larmor radius $\rho$ around the guiding center $\mathbf{X}$ yields $\rho(\mathbf{x}) \approx \rho(\mathbf{X})$. Note, that terms of order $\rho^2$, which leads to second order terms in $\rho_\star$, will get neglected due to the gyrokinetic ordering. The Larmor radius $\rho$ also depends on the velocity $\mathbf{v}$ in particle phase space [Eq. (2.2)], or the magnetic moment $\mu$ in the guiding center phase space through the formular

$$\rho(\mathbf{X}, \mu) = \frac{1}{Ze}\sqrt{\frac{2\mu m}{B(\mathbf{X})}} \ . \tag{3.11}$$

This dependence will be only used if greater clarity is needed. With result of the taylor expansion the particle position $\mathbf{x}$ can be expressed with the guiding center coordinates as

$$\mathbf{x}(\mathbf{X}, \theta) \approx \mathbf{X} + \rho(\mathbf{X})\mathbf{a}(\theta) \ . \tag{3.12}$$

The particle velocity $\mathbf{v}$ is the sum of the velocity along the magnetic field $v_\parallel$, the gyration velocity $\mathbf{v}_\perp$ and the drift velocity, which will be neglected because the particle drifts can be described by the motion of the guiding center. So to summarize the velocity $\mathbf{v}$ in the guiding center frame can be expressed as

$$\mathbf{v} = v_\parallel \mathbf{b}(\mathbf{x}) + \mathbf{v}_\perp = v_\parallel \mathbf{b}(\mathbf{x}) + \rho(\mathbf{x})\dot{\mathbf{a}}(\theta) \ . \tag{3.13}$$

Applying Taylor expansion again around the guding center $\mathbf{X}$ teh following expression can be obtained

$$\mathbf{v}(\mathbf{X}, v_\parallel, \mu, \theta) \approx v_\parallel \left[\mathbf{b}(\mathbf{X}) + \partial_{\mathbf{X}}\mathbf{b}(\mathbf{X}) \cdot \mathbf{a}(\theta)\rho(\mathbf{X}, \mu)\right] + \rho(\mathbf{X}, \mu)\dot{\mathbf{a}}(\theta) \ . \tag{3.14}$$

Now, the transformation [Eq. (3.10)] can be applied to express the fundamental one-form in the new coordinates with the following components

$$\begin{aligned}
\Gamma_{X^i} &= \gamma_{x^j}\frac{\mathrm{d}x^j}{\mathrm{d}X^i} + \gamma_{v^j}\frac{\mathrm{d}v^j}{\mathrm{d}X^i} + \gamma_t\frac{\mathrm{d}t}{\mathrm{d}X^i} = \gamma_{x^j}\frac{\mathrm{d}x^j}{\mathrm{d}X^i} & \Gamma_{v_\parallel} &= \gamma_{x^j}\frac{\mathrm{d}x^j}{\mathrm{d}v_\parallel} + \gamma_{v^j}\frac{\mathrm{d}v^j}{\mathrm{d}v_\parallel} = 0 \\
\Gamma_\mu &= \gamma_{x^j}\frac{\mathrm{d}x^j}{\mathrm{d}\mu} & \Gamma_\theta &= \gamma_{x^j}\frac{\mathrm{d}x^j}{\mathrm{d}\theta} \\
\Gamma_t &= \gamma_t\frac{\mathrm{d}t}{\mathrm{d}t} + \mu B(\mathbf{X}) = \gamma_t + \mu B(\mathbf{X}) \ .
\end{aligned} \tag{3.15}$$

Note, that to the Hamiltonian part $\Gamma_t$ the energy term of the magnetic field $B$ at the guiding center $\mathbf{X}$ has to be added, due to the circular motion of the particle around the center.

In Equation (3.15) the components of the fundamental one-form of the particle phase space $\gamma_\nu$ and the equation for $\mathbf{v}$ in guiding center coordinates [Eq. (3.14)] will be inserted and the Taylor expansion up to the first order applied for terms containing the particle position $\mathbf{x}$ as argument. After that, the gyroaveraging operator $\mathcal{G}$ will be used, which is defined as the integral over the gyrophase $\theta$

$$\mathcal{G}\{G(\mathbf{x})\} = \bar{G}(\mathbf{X}) = \frac{1}{2\pi}\int_0^{2\pi} \mathrm{d}\theta\; G(\mathbf{X} + \mathbf{r}(\theta)) \;, \tag{3.16}$$

with an example field $G(\mathbf{x})$. Due to the definition of the vector $\mathbf{a}$ [Eq. (3.9)] the first order terms in $\mathbf{a}$ and $\dot{\mathbf{a}}$ disappear under gyroaveraging. Following all the previous steps, one can obtain

$$\begin{aligned}
\bar{\Gamma}_{\mathbf{X}} &= m v_\parallel b_i(\mathbf{X}) + m u_{0i} + Ze\mathbf{A}(\mathbf{X}) & \bar{\Gamma}_{v_\parallel} &= 0 \\
\bar{\Gamma}_{\mu} &= 0 & \bar{\Gamma}_{\theta} &= \frac{2\mu m}{Ze} \\
\bar{\Gamma}_{t} &= -\left(\frac{1}{2}m v_\parallel^2 - \frac{1}{2}m u_0^2 + Ze\Phi(\mathbf{X}) + \mu B(\mathbf{X})\right) \;,
\end{aligned} \tag{3.17}$$

which results in the fundamental one-form in guiding center coordinates

$$\begin{aligned}
\bar{\Gamma} = &\left(m v_\parallel \mathbf{b}(\mathbf{X}) + m\mathbf{u}_0 + Ze\mathbf{A}(\mathbf{X})\right)\cdot \mathrm{d}\mathbf{X} + \frac{2\mu m}{Ze}\mathrm{d}\theta \\
&- \left(\frac{1}{2}m v_\parallel^2 - \frac{1}{2}m u_0^2 + Ze\Phi(\mathbf{X}) + \mu B(\mathbf{X})\right)\mathrm{d}t \;.
\end{aligned} \tag{3.18}$$

Note that as a consequence of the Lagrangian being independent of the gyrophase $\theta$, the magnetic moment $\mu$ (the associated conjugated coordinate pair of $\theta$) becomes an invariant of the motion ($\dot{\mu} = 0$).

As in Chapter 3.2.1 perturbations [Eq. (3.6)] will get introduced to the guiding center Lagrangian. The transformation of the equilibrium part is already performed above, so only the pertrubation part with the pertubated Lagrangian in the particle phase space $\gamma_1$ has to be transfromed to the guiding center phase space. The transformation is analogous to the calculation before, the key difference is that the fluctuations quantities vary on a small length scale and Taylor expansion around the guiding center $\mathbf{X}$ can not be applied advantageous. Their values have to be taken at the particle position, which is a function of the gyroangle in guiding center coordinates. After this clearification the components of the perturbated Lagrangian in the guiding center phase space can be written as

$$\begin{aligned}
\Gamma_{1,X^i} &= \gamma_{1,x^j}\frac{\mathrm{d}x^j}{\mathrm{d}X^i} & \Gamma_{1.v_\parallel} &= 0 \\
\Gamma_{1,\mu} &= \gamma_{1,x^j}\frac{\mathrm{d}x^j}{\mathrm{d}\mu} & \Gamma_{1,\theta} &= \gamma_{1,x^j}\frac{\mathrm{d}x^j}{\mathrm{d}\theta} \\
\Gamma_{1,t} &= \gamma_{1,t} \;.
\end{aligned} \tag{3.19}$$

After inserting the components of the perturbated Lagrangian $\gamma_1$ and neglecting terms of order $\rho^2$, due to gyrokinetic ordering, the pertrubated compentents in the guiding center coordinates can be expressed as

$$\begin{aligned}
\Gamma_{1,\mathbf{X}} &\approx Ze\mathbf{A}_1(\mathbf{x}) & \Gamma_{1.v_\parallel} &= 0 \\
\Gamma_{1,\mu} &= \frac{Z}{|Z|}\frac{1}{v_\perp(\mathbf{X},\mu)}\mathbf{A}_1(\mathbf{x})\cdot\mathbf{a}(\theta) & \Gamma_{1,\theta} &= \frac{Z}{|Z|}\frac{2\mu}{v_\perp(\mathbf{X},\mu)}\mathbf{A}_1(\mathbf{x})\cdot\frac{\mathrm{d}\mathbf{a}(\theta)}{\mathrm{d}\theta} \\
\Gamma_{1,t} &= -Ze\Phi_1(\mathbf{x})\ .
\end{aligned} \tag{3.20}$$

Finally, the fundamental one-form in the guiding center phase space $\Gamma$ with perturbation can be written as

$$\begin{aligned}
\Gamma &= \bar{\Gamma}_0 + \Gamma_1 \\
\bar{\Gamma}_0 &= \big(mv_\parallel\mathbf{b}(\mathbf{X}) + m\mathbf{u}_0 + Ze\mathbf{A}_0(\mathbf{X})\big)\cdot\mathrm{d}\mathbf{X} + \frac{2\mu m}{Ze}\mathrm{d}\theta \\
&\quad - \left(\frac{1}{2}mv_\parallel^2 - \frac{1}{2}mu_0^2 + Ze\Phi_0(\mathbf{X}) + \mu B_0(\mathbf{X})\right)\mathrm{d}t \\
\Gamma_1 &= Ze\mathbf{A}_1(\mathbf{x})\cdot\mathrm{d}\mathbf{X} + \frac{Z}{|Z|}\frac{1}{v_\perp}\mathbf{A}_1(\mathbf{x})\cdot\mathbf{a}\mathrm{d}\mu + \frac{Z}{|Z|}\frac{2\mu}{v_\perp}\mathbf{A}_1(\mathbf{x})\cdot\frac{\mathrm{d}\mathbf{a}}{\mathrm{d}\theta}\mathrm{d}\theta - Ze\Phi_1(\mathbf{x})\mathrm{d}t\ .
\end{aligned} \tag{3.21}$$

### 3.2.3 Lagrangian in Gyrocenter Phase Space

The transformation of the guiding center Lagrangian $\Gamma$ into the Lagrangian in gyrocenter phase space $\bar{\Gamma}$ aims to remove the gyroangle $\theta$ dependence resulting from the introduction of fluctuations. To destinguish between the guiding center and the gyrocenter coordinates all quantities associated with the gyrocenter are getting an overbar, i.e. $\bar{\Gamma}$. The new set of gyrocenter coordinates are given by $\{\bar{\mathbf{X}}, \bar{v}_\parallel, \bar{\mu}\}$, but these coordinates will not been used in this thesis. Since the derivation of fundamental the one-form in gyrocenter phase space $\bar{\Gamma}$ uses the Lie transform pertubation method, which is beyond the scopes of this thesis, the reader is referred to the Refs. 6 and 20 for more details. The Lagrangian in the gyrocenter phase space can be expressed as

$$\begin{aligned}\bar{\Gamma} &= \bar{\Gamma}_0 + \bar{\Gamma}_1 \\ &= \left(mv_\parallel \mathbf{b}_0(\mathbf{X}) + m\mathbf{u}_0 + Ze\left(\mathbf{A}_0(\mathbf{X}) + \bar{\mathbf{A}}_1(\mathbf{X})\right)\right)\cdot \mathrm{d}\mathbf{X} + \frac{2\mu m}{Ze}\mathrm{d}\theta \\ &\quad - \left(\frac{1}{2}m\left(v_\parallel^2 - u_0^2\right) + Ze\left(\Phi_0(\mathbf{X}) + \bar{\Phi}_1(\mathbf{X})\right) + \mu\left(B_0(\mathbf{X}) + \bar{B}_{1\parallel}(\mathbf{X})\right)\right)\,\mathrm{d}t\ ,\end{aligned} \tag{3.22}$$

where $B_0$ is the equilibrium magnetic field and $\bar{B}_{1\parallel}$ is the magnetic field introduced by the vector potential $\mathbf{A}_1$. Note, that the pertubations of the scalar and vector potential will be seperated into an oscillating and a gyroaveraged part which will be expressed as

$$\Phi_1 = \widetilde{\Phi}_1 + \bar{\Phi}_1 \qquad \mathbf{A}_1 = \widetilde{\mathbf{A}}_1 + \bar{\mathbf{A}}_1\ , \tag{3.23}$$

although the oscillating parts will be added to the gauge function of the Lie transformation and will not be included in the Lagrangian of the gyrocenter phase space. The quantity $\bar{B}_{1\parallel}$ is the shorter notation of following gyroaveraged quantity defined as

$$\mathcal{G}\{Ze\mathbf{A}_1(\mathbf{x})\cdot\mathbf{v}_\perp(\mathbf{X},\mu,\theta)\} = \mu\bar{B}_{1\parallel}(\mathbf{X})\ . \tag{3.24}$$

Additionally

## 3.3 Gyrokinetic Equation

### 3.3.1 Vlasov Equation

Because of the large number of particles in the fusion plasma a prediction on the basis of Newton-Maxwell dynamics results in an impossible task for simulation, but this problem can be solved with a statistical approach. For that the distribution function $f(\mathbf{x}, \mathbf{v}, t)$ in the particle phase space $\{\mathbf{x}, \mathbf{v}\}$ will be considered. Because collisions are happening at much smaller frequencies than the characteristic frequencies connected to turbulence, the collisionless model is often preferred[7] which results through evolution of the particle density distribution function in the *Vlasov equation*

$$\frac{\partial f}{\partial t} + \dot{\mathbf{x}} \cdot \frac{\partial f}{\partial \mathbf{x}} + \dot{\mathbf{v}} \cdot \frac{\partial f}{\partial \mathbf{v}} = 0 \ . \tag{3.25}$$

In the gyrocenter phase space $\{\mathbf{X}, v_\parallel, \mu\}$, the overbar introduced in Chapter 3.2.3 gets droped for simplicity for all quantities, the Vlasov equation with the gyrocenter distribution function $F$ takes the following form

$$\frac{\partial F}{\partial t} + \dot{\mathbf{X}} \cdot \frac{\partial F}{\partial \mathbf{X}} + \dot{v}_\parallel \cdot \frac{\partial F}{\partial v_\parallel} = 0 \ , \tag{3.26}$$

where the gyrophase $\theta$ is still an ignorable coordinate and the time derivative of the magnetic moment $\mu$ is zero, beacause the magnetic moment $\mu$ is an exact invariant. In Equation (3.26) the terms of the time derivative of the gyrocenter $\dot{\mathbf{X}}$ and the parallel velocity $\dot{v_\parallel}$ have to be expressed through the gyrocenter Lagrangian with the Euler-Lagrange equation. The Euler-Lagrange equation can be written as

$$\left(\frac{\partial \gamma_j}{\partial z^i} - \frac{\partial \gamma_i}{\partial z^j}\right) \frac{\mathrm{d}z^j}{\mathrm{d}t} = \frac{\partial H}{\partial z^i} + \frac{\partial \gamma_i}{\partial t} \ . \tag{3.27}$$

Inserting Equation (3.22) into the Euler-Lagrange equation and apply multiple calculations detailed in Ref. 20 the equations of motion can be obtained as

$$\begin{aligned} \dot{\mathbf{X}} &= \mathbf{b}_0 v_\parallel + \mathbf{v}_\chi + \mathbf{v}_\mathrm{D} \qquad & \dot{v}_\parallel &= \frac{\dot{\mathbf{X}}}{m v_\parallel} \cdot \Big( Ze\bar{\mathbf{E}} - \mu \nabla (B_0 + \bar{B}_{1\parallel}) + \underbrace{\frac{1}{2} m \nabla u_0^2}_{mR\Omega^2 \nabla R} \Big) \\ \dot{\mu} &= 0 & \dot{\theta} &= \omega_\mathrm{c} - \frac{Ze}{m} \partial_\mu \left( Ze\bar{\mathbf{A}}_1 \cdot \dot{\mathbf{X}} - Ze\bar{\Phi}_1 - \mu \bar{B}_{1\parallel} \right) \ , \end{aligned} \tag{3.28}$$

with the drift velocity $\mathbf{v}_\chi$ defined as the sum of the streaming velocity perpendicular to the pertubated magnetic field $\mathbf{v}_{\bar{B}_{1\perp}}$, the E × B drift in the total electric field $\mathbf{v}_{\bar{E}}$ and the grad-$B$ dirft of the parallel perturbed magnetic field $\mathbf{v}_{\nabla \bar{B}_{1\parallel}}$. The drift velocity

$\mathbf{v}_\mathrm{D}$ containing the sum of the curvature drift $\mathbf{v}_C$, the grad-$B$ drift of the equilibrium magnetic field $\mathbf{v}_{\nabla B_0}$ and the drifts due to the Coriolis force $\mathbf{v}_\mathrm{Co}$ and centrifugal force $\mathbf{v}_\mathrm{Ce}$. Note that, the term containing $u_0^2$ got replaced with Equation (2.12) with $u_0^2 = R^2\Omega^2$. The quantity $\chi$ can be expressed as

$$\chi = \underbrace{(\Phi_0 + \bar{\Phi}_1)}_{\bar{\Phi}} - v_\parallel \bar{A}_{1\parallel} + \frac{\mu}{Ze}\bar{B}_{1\parallel} \tag{3.29}$$

which results the drift velocity $\mathbf{v}_\chi$

$$\mathbf{v}_\chi = \frac{\mathbf{b}_0 \times \nabla\chi}{B_0} = \mathbf{v}_{\bar{E}} + \mathbf{v}_{\bar{B}_{1\perp}} + \mathbf{v}_{\nabla\bar{B}_{1\parallel}} \ , \tag{3.30}$$

with $\mathbf{b}_0 \times (\nabla A_{1\parallel}) \approx \nabla \times (A_{1\parallel}\mathbf{b}_0) = \mathbf{B}_{1\perp}$. The total electric field $\bar{\mathbf{E}}$ is defined as

$$\bar{\mathbf{E}} = -\nabla\bar{\Phi} - \partial_t\bar{\mathbf{A}}_1 = -\nabla\bar{\Phi} - \partial_t\left(\mathbf{b}_0 \cdot \bar{A}_{1\parallel} + \bar{\mathbf{A}}_{1\perp}\right) \ . \tag{3.31}$$

Since the time derivative of the vector potential $\partial_t\bar{\mathbf{A}}_1$ is one order smaller as the gradient of the electrostatic potential $\nabla\bar{\Phi}$, due to normalization assumptions in gyrokinetics[14], the contribution of the vector potential will be neglected in the $\mathbf{v}_{\bar{E}}$ velocity term.

### 3.3.2 The delta-*f* Approximation

The delta-*f* approximation separates the density distrubution function $F$ into an equilibrium part $F_0$ and pertubation part $F_1$, i.e. $F = F_0 + F_1$. Applying the delta-*f* approximation on the gyrocenter Vlasov equation leads to

$$\frac{\partial F_1}{\partial t} + \dot{\mathbf{X}} \cdot \nabla F_1 + \dot{v}_\parallel \cdot \frac{\partial F_1}{\partial v_\parallel} = \underbrace{-\dot{\mathbf{X}} \cdot \nabla F_0 - \dot{v}_\parallel \frac{\partial F_0}{\partial v_\parallel}}_{S} , \tag{3.32}$$

with the source term $S$. Substituting from Equation (3.28) the equations for $\dot{\mathbf{X}}$ and $\dot{v}_\parallel$ into the delta-*f* approximated Vlasov equation results in

$$\frac{\partial F_1}{\partial t} + \dot{\mathbf{X}} \cdot \nabla F_1 - \frac{\mathbf{b}_0}{m} \cdot \left( Ze\nabla\Phi_0 + \mu\nabla B_0 - mR\Omega^2\nabla R \right) \cdot \frac{\partial F_1}{\partial v_\parallel} = S \, . \tag{3.33}$$

Note that only the terms of order $\rho_\star$ has to be kept in $\dot{v}_\parallel \partial_{v_\parallel} F_1$, which results in neglecting the drift velocities $\mathbf{v}_\chi$ and $\mathbf{v}_\mathrm{D}$ and the contribution of $\bar{B}_{1\parallel}$ and $\bar{\Phi}_1$, since these terms are after calculation of order $\rho_\star^2$.

The equilibrium distribution fuction $F_0$ is assumed to be a Maxwellian which includes a finite equilibrium electric field $\Phi_0$ to balance the centrifugal force (in the co-rotating frame) due toridial rotation of the plasma.
In the rotating frame the included energy term can be written as

$$\mathcal{E} = Ze\langle\Phi_0\rangle - \frac{1}{2} m\omega_\varphi^2 \left( R^2 - R_0^2 \right) \ , \tag{3.34}$$

where $\langle \cdot \rangle$ denote flux-surface averaging, $\omega_\varphi$ the plasma rotation frequency [Eq. (2.13)], $R$ the local major radius and $R_0$ is an integration constant which can be chosen, i.e. major radius of the plasma or flux surface average of the major radius. The Maxwellian is given by the following expression

$$F_0 = F_\mathrm{M}(\mathbf{X}, v_\parallel, \mu) = \frac{n_{R_0}}{(2\pi T/m)^{3/2}} \exp\left( -\frac{\frac{1}{2}m(v_\parallel - u_\parallel)^2 + \mu B_0 + \mathcal{E}}{T} \right) \ , \tag{3.35}$$

where $n_{R_0}$ is the particle density at the position $R = R_0$ and is related to equilibrium particle density through the relation $n_0 = n_{R_0} \exp(-\mathcal{E}/T)$.[16]
Furthermore, $u_\parallel$ is the rotation speed of the plasma in the rotating frame parallel to the magnetic field [Eq. (2.14)]. The Maxwellian can seperated in

$$F_\mathrm{M}(\mathbf{X}, v_\parallel, \mu) = F_\mathrm{M}(v_\parallel) F_\mathrm{M}(\mu) e^{-\mathcal{E}/T}, \tag{3.36}$$

$$F_\mathrm{M}(v_\parallel) = \frac{n_{R_0}}{(2\pi T/m)^{3/2}} \exp\left( -\frac{\frac{1}{2}m(v_\parallel - u_\parallel)^2}{T} \right) \qquad F_\mathrm{M}(\mu) = \exp\left( -\frac{\mu B_0}{T} \right) \ . \tag{3.37}$$

The derivatives of the Maxwellian can be expressed as

$$\begin{aligned}\nabla F_{\mathrm{M}} = &\left[\frac{\nabla n_{R_0}}{n_{R_0}} + \left(\frac{\frac{1}{2}mv_\parallel^2 + \mu B_0 + \mathcal{E}}{T} - \frac{3}{2}\right)\frac{\nabla T}{T} - \frac{\mu B_0}{T}\frac{\nabla B_0}{B_0}\right.\\ &\left. + \left(\frac{mv_\parallel R B_{\mathrm{t}}}{BT} + m\omega\left(R^2 - R_0^2\right)\right)\nabla\omega_\varphi\right] F_{\mathrm{M}}\\ \partial_{v_\parallel} F_{\mathrm{M}} = &-\frac{mv_\parallel}{T}F_{\mathrm{M}}\\ \partial_\mu F_{\mathrm{M}} = &-\frac{B_0}{T}F_{\mathrm{M}}\ ,\end{aligned} \tag{3.38}$$

where the $\nabla\omega_\varphi$ terms are the result of the derivatives of the parallel rotation velocity $u_\parallel$ and rotation energy $\mathcal{E}$ evaluated at zero rotation speed locally in the co-rotating frame.[16] It can be shown with Equations (3.28) and (3.38) that the $\nabla B_0$ term in $-\dot{\mathbf{X}}\cdot\nabla F_{\mathrm{M}}$ cancels with $(\dot{\mathbf{X}}/mv_\parallel)\mu\nabla B_0\partial_{v_\parallel}F_{\mathrm{M}}$ for purely torodial rotation. Finally, the source term can than be written as

$$\begin{aligned}S = &-(\mathbf{v}_\chi + \mathbf{v}_{\mathrm{D}})\cdot\widetilde{\nabla}F_{\mathrm{M}} - \frac{Zev_\parallel}{T}\partial_t\bar{A}_{1\parallel}F_{\mathrm{M}}\\ &-\frac{F_{\mathrm{M}}}{T}(v_\parallel\mathbf{b}_0 + \mathbf{v}_{\mathrm{D}} + \mathbf{v}_{\bar{B}_{1\perp}})\cdot(Ze\nabla\bar{\Phi} + \mu\nabla\bar{B}_{1\parallel})\ ,\end{aligned} \tag{3.39}$$

where $\widetilde{\nabla}$ referres to only the $\nabla n_{R_0}$, $\nabla T$ and $\nabla\omega_\varphi$ terms of $\nabla F_{\mathrm{M}}$.

CHAPTER

# 4

# Gyrokinetic Field Equations

## 4.1 Maxwell's Equations

To obtain a closed system the Vlasov equation gets combined with the Maxwell equations to calculate the pertubated electromagnetic fields. As usual in fusion plasma the Gauss law gets replaced by the quasi neutrality condition which implies that any deviation from neutrality can only happen on small length scales within the Debye lenght and on a timescale much shorter than that of the fluctuations. Due to non-relativistic timescale of the turbulence the dissplacement current in Ampere's law gets also neglected. Taking everything into account the Maxwell's equations can be written as

$$\begin{aligned} \sum_s Z_s e\, n_s = 0 \qquad & \nabla \times \mathbf{E}_1 = -\frac{\partial \mathbf{B}_1}{\partial t} \\ \nabla \cdot \mathbf{B}_1 = 0 \qquad & \nabla \times \mathbf{B}_1 = \mu_0 \sum_s \mathbf{j}_s \ , \end{aligned} \tag{4.1}$$

where the index $s$ refers to the species of particles, i.e. proton or electron and $\sum_s$ means that all species will be taken into account. For simplicity of the derivation the "s" index gets droped if not explicitly needed. The Maxwell's equation contain densities $n$ and currents $\mathbf{j}$ of part icles which can be expressed through the moments of the particle phase space distribution function $f$ as follows

$$\begin{aligned} n(\mathbf{x}) &= \int \mathrm{d}\mathbf{v}\ f(\mathbf{x}, \mathbf{v}) \\ j_\parallel &= Ze \int \mathrm{d}\mathbf{v}\ v_\parallel f(\mathbf{x}, \mathbf{v}) \\ \mathbf{j}_\perp &= Ze \int \mathrm{d}\mathbf{v}\ \mathbf{v}_\perp f(\mathbf{x}, \mathbf{v}) \ . \end{aligned} \tag{4.2}$$

## 4.2 Pull Back Operation into the Guiding Center Phase Space

Since the Vlasov equations [Eq. (3.33)] describes the evolution of the distribution function in the gyrocenter phase space $F$, the particle moments will be expressed with the guiding center phase space distribution function $F^{\mathrm{gc}}$ and which itself will be described through the gyrocenter distrubution function $F$ by performing a pull back from $F$ to the guiding center phase space. A schemamtic about the general idea can be seen in Figure 4.1. The pull back will be performed with the pull back operator $\mathcal{P}$ which results in

$$F^{\mathrm{gc}} = \mathcal{P}\left\{F\right\} = F \underbrace{-\frac{F_{\mathrm{M}}}{T}\left(Ze\widetilde{\Phi}_1 - \mu \bar{B}_{1\parallel}\right)}_{\text{Correction Term}}, \tag{4.3}$$

where $\widetilde{\Phi}_1$ donates to the oscillating part of the pertubation $\Phi_1$. Here, the correction term contain the fluctuations of the electro-magnetic fields and describes physically the polarization and magnetization effects of the fluctuations on the gyro orbit.[2]


Figure 4.1: Idea of gyrokinetic Maxwell's equations: The particle density $n(\mathbf{x})$, the current density $\mathbf{j}(\mathbf{x})$ and the gyrocenter distribution function $F$ are expressed in the guiding center phase space.

The particle density $n$ and currents $\mathbf{j}$ of one species can be expressed with the guiding center distribution function $F^{\mathrm{gc}}$ as

$$\begin{aligned}
n &= \int \mathrm{d}\mathbf{v}\ f(\mathbf{x},\mathbf{v}) = \frac{B_0}{m}\int \mathrm{d}\mathbf{X}\mathrm{d}v_\parallel \mathrm{d}\theta \mathrm{d}\mu\ \delta(\mathbf{X}+\mathbf{r}-\mathbf{x})F^{\mathrm{gc}} \\
j_\parallel &= Ze\int \mathrm{d}\mathbf{v}\ v_\parallel f(\mathbf{x},\mathbf{v}) = \frac{ZeB_0}{m}\int \mathrm{d}\mathbf{X}\mathrm{d}v_\parallel \mathrm{d}\theta \mathrm{d}\mu\ \delta(\mathbf{X}+\mathbf{r}-\mathbf{x})v_\parallel F^{\mathrm{gc}} \\
\mathbf{j}_\perp &= Ze\int \mathrm{d}\mathbf{v}\ \mathbf{v}_\perp f(\mathbf{x},\mathbf{v}) = \frac{ZeB_0}{m}\int \mathrm{d}\mathbf{X}\mathrm{d}v_\parallel \mathrm{d}\theta \mathrm{d}\mu\ \delta(\mathbf{X}+\mathbf{r}-\mathbf{x})\mathbf{v}_\perp F^{\mathrm{gc}}\ ,
\end{aligned} \tag{4.4}$$

where $B_0/m$ is the Jacobian of the guiding center coordinates. The delta function $\delta$ appears due to the change of coordinates and gurantees that the spatial region taken into account in the integral remains unchanged during the coordinate transformation. Physically, the delta function $\delta$ expresses that all particles which have a Larmor orbit crossing a given point $\mathbf{x}$ in the real space contribute to the particle density [Fig. 4.2].

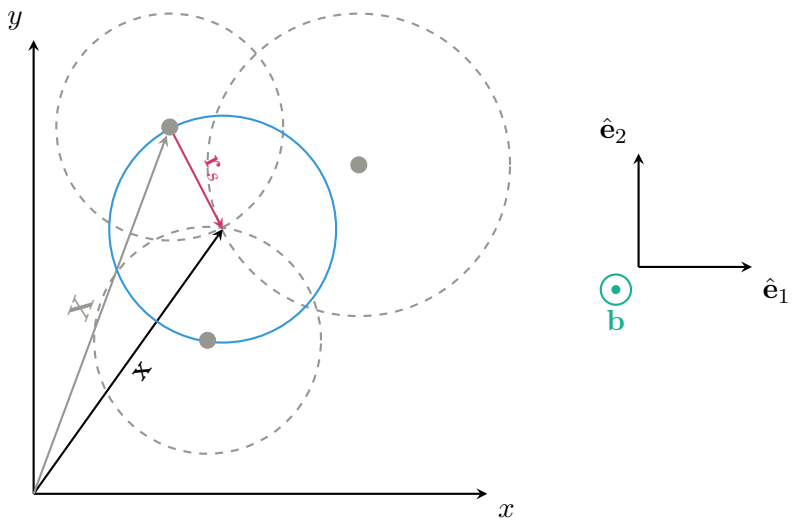


Figure 4.2: Connection between density of particles $n_s(\mathbf{x})$ and density of guiding centers: Gyro orbits with different guiding center $\mathbf{X}$ (gray dashed circles) can cross in postion $\mathbf{x}$, such that the respective gyrating particles add to the particle density $n_s$ there. For a fixed Larmor radius $\rho_s = |\mathbf{r}_s| = |\rho_s \mathbf{a}|$ (red) the particle density $n_s$ at $\mathbf{x}$ is obtained by collecting the contributions of all guiding centers on a circle with radius $\rho_s$ centered at position $\mathbf{x}$ (blue circle).

## 4.3 Gyrooperator $\mathcal{G}$

As stated in Chapter 3.2.2 the gyrooperator $\mathcal{G}$ averages over the gyrophase $\theta$ which is mostly used in the derivation of the Vlasov equation and is defined as

$$\mathcal{G}\{G(\mathbf{x})\} = \bar{G}(\mathbf{X}) = \frac{1}{2\pi}\int_0^{2\pi} \mathrm{d}\theta\ G(\mathbf{X} + \mathbf{r}(\theta)) \ . \tag{4.5}$$

To derive the field equations a second kind of gyrooperator will be introduced as

$$\mathcal{G}^\dagger\{G(\mathbf{X})\} = \langle G\rangle(\mathbf{x}) = \frac{1}{2\pi}\int_0^{2\pi} \mathrm{d}\mathbf{X}\mathrm{d}\theta\ \delta(\mathbf{X} + \mathbf{r}(\theta) - \mathbf{x})G(\mathbf{X}) \ , \tag{4.6}$$

where $\mathcal{G}^\dagger$ the hermitian conjugate of $\mathcal{G}$[21] and the delta function $\delta$ originates from the pull back operation from Chapter **??**.[11] Furthermore, the double gyroaverage operator is defined as

$$\mathcal{G}^\dagger\big\{\mathcal{G}\{G(\mathbf{x})\}\big\} = \langle\bar{G}\rangle(\mathbf{x}) = \frac{1}{(2\pi)^2}\int_0^{2\pi} \mathrm{d}\theta \int_0^{2\pi} \mathrm{d}\theta'\ G(\mathbf{X} - \mathbf{r}(\theta) + \mathbf{r}(\theta')) \ , \tag{4.7}$$

which performs a gyroaverage of the field value at all gyrocenter positions $\mathbf{X}$ with particle position $\mathbf{x}$ in their trajectory.[10]

In the case of local simulations the gyrooperators $\mathcal{G}$ and $\mathcal{G}^\dagger$ simplies to

$$\begin{aligned} \bar{\mathbf{G}}(\mathbf{x}) &= J_0(\lambda)\mathbf{G}(\mathbf{X}) \\ \langle\mathbf{G}(\mathbf{X})\rangle &= J_0(\lambda)\mathbf{G}(\mathbf{x}) \end{aligned} \tag{4.8}$$

with $J_0$ as the zeroth order Bessel function. Note, that $\bar{B}_{1\parallel}(\mathbf{X}) = -I_1(\lambda)\mu B_{1\parallel}(\mathbf{X})$, where $I_1$ is the modified first order Bessel function of first kind defined as $I_1(\lambda) = 2/\lambda\, J_1(\lambda)$. To obtain Equation (4.8) the process of gyroaveraging will be performend in the Fourier space as follows

$$\begin{aligned} \bar{\mathbf{G}}(\mathbf{x}) = \bar{\mathbf{G}}(\mathbf{X} + \mathbf{r}) &= \mathcal{G}\left\{\int \mathrm{d}\mathbf{k}\ \hat{\mathbf{G}}(\mathbf{k})e^{i\mathbf{k}\cdot(\mathbf{X}+\mathbf{r})}\right\} \\ &= \frac{1}{2\pi}\int_0^{2\pi}\mathrm{d}\theta\ \int \mathrm{d}\mathbf{k}\ \hat{\mathbf{G}}(\mathbf{k})e^{i\mathbf{k}\cdot\mathbf{X}}e^{ik_\perp\rho\cos\theta} \\ &= \int \mathrm{d}\mathbf{k}\ \hat{\mathbf{G}}(\mathbf{k})e^{i\mathbf{k}\cdot\mathbf{X}}\underbrace{\frac{1}{2\pi}\int_0^{2\pi}\mathrm{d}\theta\ e^{ik_\perp\rho\cos\theta}}_{J_0(\rho k_\perp)} \\ &= \int \mathrm{d}\mathbf{k}\ J_0(\rho k_\perp)\hat{\mathbf{G}}(\mathbf{k})e^{i\mathbf{k}\cdot\mathbf{X}} = J_0(\lambda)\mathbf{G}(\mathbf{X}) \ , \end{aligned} \tag{4.9}$$

where the wave vector $\mathbf{k}$ is defined as $\mathbf{k} = \hat{e}_1 k_\perp$. The argument $\lambda$ is given by $i\rho\nabla_\perp$ which is the inverse Fourier transformated expression of $\rho k_\perp$. The same routine can be applied

for the gyrooperator $\mathcal{G}^\dagger$ with the same result. In general the Bessel function and modified Bessel function is defined as[6]

$$\begin{aligned} J_n(z) &= \left(\frac{z}{2}\right)^n \underbrace{\sum_{\nu=0}^{\infty} \frac{\left(\left(-1/4z^2\right)^\nu\right)}{\nu!(1+\nu)!}}_{I_n(z)} , \\ J_n(z) &= \frac{i^{-n}}{\pi} \int_0^\pi \mathrm{d}\theta \; e^{iz\cos\theta} \cos(n\theta) \; . \end{aligned} \tag{4.10}$$

## Integrals with Bessel Function

In the upcoming section there will be often integrals which contain the zeroth Besselfunction $J_0(\lambda)$ and the modified Besselfunctions $I_1(\lambda)$. In general this types of integrals have the form

$$\int \mathrm{d}v_\parallel \mathrm{d}\mu \; \mu^n J_0^{2-n}(\lambda) I_1^n(\lambda) F_\mathrm{M}, \tag{4.11}$$

wuth the natural number $n = \{0, 1, 2\}$. Equation (4.11) can be seperated together with the Maxwellian [Eq. (3.37) with $u_\parallel = 0$, because of reference system to

$$e^{-\mathcal{E}/T} \int \mathrm{d}v_\parallel \; F_\mathrm{M}(v_\parallel) \int \mathrm{d}\mu \; \mu^n J_0^{2-n}(\lambda) I_1^n(\lambda) F_\mathrm{M}(\mu) \; . \tag{4.12}$$

The first integral appears in the following types

$$\begin{aligned} &1) \int \mathrm{d}v_\parallel \; F_\mathrm{M}(v_\parallel) && = \frac{n_{R_0} m}{2\pi T} \\ &2) \int \mathrm{d}v_\parallel \; v_\parallel F_\mathrm{M}(v_\parallel) && = 0 \qquad \text{(Due to symmetry)} \\ &3) \int \mathrm{d}v_\parallel \; v_\parallel^2 F_\mathrm{M}(v_\parallel) && = \frac{n_{R_0}}{2\pi} \end{aligned} \tag{4.13}$$

and the last integral occurs in three types

$$\begin{aligned} &1) \int \mathrm{d}\mu \; J_0^2(\lambda) F_\mathrm{M}(\mu) && = \frac{T}{B_0} \Gamma_0(b) \\ &2) \int \mathrm{d}\mu \; \mu J_0(\lambda) I_1(\lambda) F_\mathrm{M}(\mu) && = \frac{T^2}{B_0^2} (\Gamma_0(b) - \Gamma_1(b)) \\ &3) \int \mathrm{d}\mu \; \mu^2 I_1^2(\lambda) F_\mathrm{M}(\mu) && = \frac{T^3}{B_0^3} 2(\Gamma_0(b) - \Gamma_1(b)) \; , \end{aligned} \tag{4.14}$$

with the notation $\Gamma_n(b) = I_n(b) e^{-b}$ with the modified Bessel function $I_n$ [Eq. (4.10)] and $b = -\rho_\mathrm{th}^2 \nabla^2{}_\perp$. $\rho_\mathrm{th}$ referres the thermal Larmor radius [Eq. (2.4)].[20]

## 4.4 Normalization

To implement the field equations into the local version of **GKW** , one has to normalize the quantities in the equations. This section is based on Ref. 14. The reference values are indicated by the index "ref", the dimensionless noramlized by "N" and the relative dimensionless values by the index "R". This section is based on Ref 4, 20 and 14.

A reference mass $m_{\rm ref}$, density $n_{\rm ref}$, temperature $T_{\rm ref}$, magnetic field $B_{\rm ref}$ and major radius $R_{\rm ref}$ is chosen. With these quantities the reference thermal velocity $v_{\rm th,ref}$ and reference thermal Larmor radius $\rho_{\rm th,ref}$ gets defines as

$$T_{\rm ref} = \frac{1}{2} m_{\rm ref} v_{\rm th,ref}^2 \qquad \rho_{\rm th,ref} = \frac{m_{\rm ref} v_{\rm th,ref}}{e B_{\rm ref}} = \frac{2 T_{\rm ref}}{e B_{\rm ref} v_{\rm th,ref}} \qquad \rho_\star = \frac{\rho_{\rm th,ref}}{R_{\rm ref}}$$

and for convenience reason the small parameter $\rho_\star$ got redefined.

- **Relative Quantities:**

$$m = m_{\rm ref} m_{\rm R} \qquad n_{R_0} = n_{\rm ref} n_{\rm R} \qquad T = T_{\rm ref} T_{\rm R} \qquad v_{\rm th} = v_{\rm th,ref} v_{\rm thR}$$

- **Normalized Quantities:**

$$R = R_{\rm ref} R_{\rm N} \qquad B_0 = B_{\rm ref} B_{\rm N} \qquad \mu = \frac{2 T_{\rm ref} T_{\rm R}}{B_{\rm ref}} \mu_{\rm N} \qquad v_\parallel = v_{\rm th} v_{\parallel \rm N}$$

$$k = \frac{k_{\rm N}}{\rho_\star} \qquad k_\parallel = \frac{k_{\parallel \rm N}}{\rho_\star} \qquad k_\perp = \frac{k_{\perp \rm N}}{\rho_{\rm th,ref}}$$

$$\beta = \beta_{\rm ref} \beta_{\rm N} \qquad \beta_{\rm ref} = \frac{2 \mu_0 n_{\rm ref} T_{\rm ref}}{B_{\rm ref}^2}$$

  - **Fluctuating Fields:**

$$\Phi_1 = \rho_\star \frac{T_{\rm ref}}{e} \Phi_{1\rm N} \qquad B_{1\parallel} = \rho_\star B_{\rm ref} B_{1\parallel \rm N}$$

$$A_{1\parallel} = B_{\rm ref} R_{\rm ref} \rho_\star^2 A_{1\parallel \rm N} \qquad E_{1\parallel} = \frac{2 T_{\rm ref}}{e} \frac{1}{R_{\rm ref}} \rho_\star E_{1\parallel \rm N}$$

  - **Time, Frequency and Centrifugal Energy:**

$$t = \frac{R_{\rm ref}}{v_{\rm th,ref}} t_{\rm N} \qquad \Omega = \frac{v_{\rm th,ref}}{R_{\rm ref}} \Omega_{\rm N} \qquad \mathcal{E} = T_{\rm ref} \mathcal{E}_{\rm N}$$

  - **Distrubution Function and Vlasov Equation:**

$$F = \rho_\star \frac{n_{R_0}}{v_{\rm th}^3} F_{\rm N} \qquad F_{\rm M} = \frac{n_{R_0}}{v_{\rm th}^3} F_{\rm MN} \qquad \mathcal{V} = \rho_\star \frac{v_{\rm th,ref}}{R_{\rm ref}} \frac{n_{R_0}}{v_{\rm th}^3} \mathcal{V}_{\rm N}$$

  - **Gradients:**

$$\nabla_\perp = \frac{1}{R_{\rm ref}} \nabla_{\perp \rm N} \qquad \nabla_\parallel = \frac{1}{R_{\rm ref}} \nabla_{\parallel \rm N} \ .$$

## 4.5 Field Equations

### 4.5.1 Coulomb's Law - Perturbated Electrostatic Potential $\Phi_1$

To evaluate the pertrubated electrostatic potential $\Phi_1$ the modified guiding center distribution function $F^{\text{gc}}$ [Eq. (4.3)] gets inserted into the equation for the particle density $n(\mathbf{x})$ which results in

$$\begin{aligned} n_1(\mathbf{x}) &= \frac{B_0}{m}\int \mathrm{d}\mathbf{X}\mathrm{d}v_\parallel \mathrm{d}\theta\mathrm{d}\mu\ \delta(\mathbf{X}+\mathbf{r}-\mathbf{x})\left(F_1 - \frac{F_\mathrm{M}}{T}\left(Ze\widetilde{\Phi}_1 - \mu\bar{B}_{1\parallel}\right)\right) \\ &= \bar{n}_1(\mathbf{x}) + n_{\mathcal{P}}(\mathbf{x})\ , \end{aligned} \tag{4.15}$$

with the density of the gyrocenter $\bar{n}_1(\mathbf{x})$ and the variations on the gyro orbit to the particle density $n_{\mathcal{P}}(\mathbf{x})$ which describes the polarization effects of the fluctuating fields on the gyro orbit[2]. The gyrocenter density can be simplyfied with the gyroperator $\mathcal{G}^\dagger$ [Eq. (4.6)] to

$$\bar{n}_1(\mathbf{x}) = \frac{B_0}{m}\int \mathrm{d}\mathbf{X}\mathrm{d}v_\parallel\mathrm{d}\theta\mathrm{d}\mu\ \delta(\mathbf{X}+\mathbf{r}-\mathbf{x})F_1 = \frac{2\pi B_0}{m}\int \mathrm{d}v_\parallel\mathrm{d}\mu\ \langle F_1\rangle\ . \tag{4.16}$$

The polarization density $n_{\mathcal{P}}$ is given by

$$n_{\mathcal{P}}(\mathbf{x}) = -\frac{2\pi B_0}{m}\int \mathrm{d}v_\parallel\mathrm{d}\mu\ \frac{F_\mathrm{M}}{T}\left(Ze\left(\Phi_1(\mathbf{x}) - \langle\bar{\Phi}_1\rangle(\mathbf{x})\right) - \mu\langle\bar{B}_{1\parallel}\rangle\right)\ , \tag{4.17}$$

where $n_{R_0}$ is a background density and $T$ is a background temperature. To derive the term for the polarization density $n_{\mathcal{P}}$ the oscillating Part of the electro static potential got replaced with $\widetilde{\Phi}_1(\mathbf{X}+\mathbf{r}) = \Phi_1(\mathbf{X}+\mathbf{r}) - \bar{\Phi}_1(\mathbf{X})$ and the gyrooperator $\mathcal{G}^\dagger$ were used. Taking everything into account and insert it into the quaisneutrality equation $\sum_s Z_s e\, n_{1,s} = 0$ the field equation for the perturbated electrostatic potential $\Phi_1$ is given by

$$\begin{aligned} &\sum_s \frac{Z_s^2 e^2}{m_s}\int \mathrm{d}v_\parallel\mathrm{d}\mu\ \frac{F_{\mathrm{M},s}}{T_s}\left(\Phi_1(\mathbf{x}) - \langle\bar{\Phi}_1\rangle(\mathbf{x})\right) = \\ &\sum_s \frac{Z_s e}{m_s}\int \mathrm{d}v_\parallel\mathrm{d}\mu\ \langle F_{1,s}\rangle + \frac{F_{\mathrm{M},s}}{T_s}\mu\langle\bar{B}_{1\parallel}\rangle\ . \end{aligned} \tag{4.18}$$

With the use of the local gyrooperator $\mathcal{G}$ the density of the gyrocenter $\bar{n}_1$ and the polarization density $n_{\mathcal{P}}$ can be expressed as

$$\bar{n}_1(\mathbf{x}) = \frac{2\pi B_0}{m}\int \mathrm{d}v_\parallel\mathrm{d}\mu\ J_0(\lambda)F_1(\mathbf{x}, v_\parallel, \mu)\ , \tag{4.19}$$

$$\begin{aligned} n_{\mathcal{P}}(\mathbf{x}) =& \frac{Zen_{R_0}(\mathbf{x})}{T}e^{-\mathcal{E}/T}(\Gamma_0(b)-1)\Phi_1(\mathbf{x}) \\ &+ n_{R_0}(\mathbf{x})e^{-\mathcal{E}/T}(\Gamma_0(b)-\Gamma_1(b))\frac{B_{1\parallel}(\mathbf{x})}{B_0}\ , \end{aligned} \tag{4.20}$$

where $n_{R_0}$ is the background density at postion $R_0$ and $T$ is the background temperature. To derive the term for the polarization density $n_{\mathcal{P}}$ the integrals mentioned in Chapter 4.3 were performed. The field equation for the perturbated electrostatic potential $\Phi_1$ in the local simulation is given by

$$\begin{aligned} &\sum_s \frac{Z_s^2 e^2}{T_s} n_{R_0,s} e^{-\mathcal{E}_s/T_s} \left(1 - \Gamma_0(b_s)\right) \Phi_1(\mathbf{x}) = \\ &\sum_s Z_s e \left( \bar{n}_{1,s} + n_{R_0,s} e^{-\mathcal{E}_s/T_s} (\Gamma_0(b_s) - \Gamma_1(b_s)) \frac{B_{1\parallel}(\mathbf{x})}{B_0} \right) \end{aligned} \tag{4.21}$$

and takes the following form after performing the Fourier-transform and applying the normalizing expressions [Ch. **??**]

$$\begin{aligned} &\sum_s Z_s n_{\mathrm{R},s} e^{-\mathcal{E}_{\mathrm{N},s}/T_{\mathrm{R},s}} \left(1 - \Gamma_0(b_s)\right) \frac{Z_s}{T_{\mathrm{R},s}} \widehat{\Phi}_{1\mathrm{N}} = \\ &\sum_s Z_s n_{\mathrm{R},s} 2\pi B_{\mathrm{N}} \int \mathrm{d}v_{\parallel\mathrm{N}} \mathrm{d}\mu_{\mathrm{N}} \; J_0(k_\perp \rho_s) \widehat{F}_{1\mathrm{N},s} \\ &+ \sum_s Z_s n_{\mathrm{R},s} e^{-\mathcal{E}_{\mathrm{N},s}/T_{\mathrm{R},s}} (\Gamma_0(b_s) - \Gamma_1(b_s)) \frac{\widehat{B}_{1\parallel\mathrm{N}}}{B_{\mathrm{N}}} \end{aligned} \tag{4.22}$$

### 4.5.2 Plasma Compression - Perturbated Parallel Magnetic Field $B_{1\parallel}$

The perpendicular compentent of Ampere's law can be written as

$$(\nabla \times B_{1\parallel})_\perp = \begin{pmatrix} \partial_y B_{1\parallel} - \partial_z B_{1y} \\ \partial_z B_{1x} - \partial_x B_{1\parallel} \end{pmatrix} = \mu_0 \mathbf{j}_{1\perp} \ , \tag{4.23}$$

where $z$ is the direction of the equilibrium magnetic field $B_0$. The parallel gradients of the pertrubated magnetic field can be neglegted since they are one order smaller than the perpendicular ones, which results in

$$\begin{pmatrix} \partial_y B_{1\parallel} \\ -\partial_x B_{1\parallel} \end{pmatrix} = \nabla_\perp B_{1\parallel} \times \mathbf{b} = \mu_0 \mathbf{j}_{1\perp} \ . \tag{4.24}$$

After performing the pull back operation the perpendicular current $\mathbf{j}_{1\perp}$ is given by

$$\mathbf{j}_{1\perp} = \frac{ZeB_0}{m} \int \mathrm{d}\mathbf{X} \mathrm{d}v_\parallel \mathrm{d}\theta \mathrm{d}\mu \ \delta(\mathbf{X} + \mathbf{r} - \mathbf{x}) \mathbf{v}_\perp \left( F_1 - \frac{F_\mathrm{M}}{T} \left( Ze\widetilde{\Phi}_1 - \mu \bar{B}_{1\parallel} \right) \right) \ . \tag{4.25}$$

Inserting the pertrubated perpenedicular current $\mathbf{j}_{1\perp}$ into Ampere's law and apply the same method as in Ref 20 results in the field equation for the pertrubated parallel magnetic field $B_{1\parallel}$ which can be expressed as

$$\begin{aligned} &\left( 1 + \sum_s \beta_s (\Gamma_0(b_s) - \Gamma_1(b_s)) e^{-\mathcal{E}_s/T_s} \right) B_{1\parallel} = \\ &- \sum_s \frac{2\pi\mu_0 B_0}{m_s} \int \mathrm{d}v_\parallel \mathrm{d}\mu \ \mu I_n(\lambda_s) F_{1,s} \\ &- \sum_s (\Gamma_0(b_s) - \Gamma_1(b_s)) e^{-\mathcal{E}_s/T_s} \frac{Z_s e \mu_0 n_{R_0,s}}{B_0} \Phi_1 \ , \end{aligned} \tag{4.26}$$

with $\beta_s$ as the plasma beta of a given species. Fourier transformation and normalization with $\beta = \beta_\mathrm{ref} \beta_\mathrm{N}$ yields

$$\begin{aligned} &\left( 1 + \sum_s \frac{T_{\mathrm{R},s} n_{\mathrm{N},s}}{B_\mathrm{N}^2} \beta_\mathrm{ref} (\Gamma_0(b_s) - \Gamma_1(b_s)) e^{-\mathcal{E}_{\mathrm{N},s}/T_{\mathrm{R},s}} \right) \widehat{B}_{1\parallel\mathrm{N}} = \\ &- \sum_s \beta_\mathrm{ref} 2\pi B_\mathrm{N} T_{\mathrm{R},s} n_{\mathrm{R},s} \int \mathrm{d}v_{\parallel\mathrm{N}} \mathrm{d}\mu_\mathrm{N} \ \mu_\mathrm{N} I_1(k_\perp \rho_s) \widehat{F}_{1\mathrm{N},s} \\ &- \sum_s \beta_\mathrm{ref} (\Gamma_0(b_s) - \Gamma_1(b_s)) e^{-\mathcal{E}_{\mathrm{N},s}/T_{\mathrm{R},s}} \frac{Z_s n_{\mathrm{R},s}}{2B_\mathrm{N}} \widehat{\Phi}_{1\mathrm{N}} \ . \end{aligned} \tag{4.27}$$

### 4.5.3 Ampere's Law - Plasma Induction $A_{1\parallel}$

To express the parallel pertrubation of the vector potential *Apar*, i.e. the plasma induction, the method is analogous to Chapter 4.5.1. Using the Coulomb gauge $\nabla \cdot \mathbf{A}_1 = 0$ in the parallel compentent of Ampere's law results in

$$\nabla^2 A_{1\parallel} = -\mu_0 j_{1\parallel} = -\mu_0 \sum_s j_{1\parallel,s} \ . \tag{4.28}$$

Performing the pull back one last time the parallel perturbation of the current density $j_{1\parallel}$ is given by

$$\begin{aligned} j_{1\parallel} &= \frac{ZeB_0}{m} \int \mathrm{d}\mathbf{X}\mathrm{d}v_\parallel \mathrm{d}\theta \mathrm{d}\mu \ \delta(\mathbf{X} + \mathbf{r} - \mathbf{x}) v_\parallel \left( F_1 - \frac{F_\mathrm{M}}{T} \left( Ze\widetilde{\Phi}_1 - \mu \bar{B}_{1\parallel} \right) \right) \\ &= \frac{ZeB_0}{m} \int \mathrm{d}\mathbf{X}\mathrm{d}v_\parallel \mathrm{d}\theta \mathrm{d}\mu \ \delta(\mathbf{X} + \mathbf{r} - \mathbf{x}) v_\parallel F_1 \\ &= \frac{2\pi ZeB_0}{m} \int \mathrm{d}v_\parallel \mathrm{d}\mu \ \langle v_\parallel F_1 \rangle \ , \end{aligned} \tag{4.29}$$

although the term $v_\parallel F_\mathrm{M}$ vanishes during the integration along $v_\parallel$, due to symmetry of the Maxwellian $F_\mathrm{M}$. Inserting Equation (4.29) into Ampere's law yields the field equation for the plasma induction as follows

$$\nabla^2 A_{1\parallel} = -\sum_s \frac{2\pi Z_s e \mu_0 B_0}{m_s} \int \mathrm{d}v_\parallel \mathrm{d}\mu \ \langle v_\parallel F_{1,s} \rangle \ . \tag{4.30}$$

The field equation for the plasma induction follows simply after the use of the local gyroperator and is given by

$$\nabla^2 A_{1\parallel} = -\sum_s \frac{2\pi Z_s e \mu_0 B_0}{m_s} \int \mathrm{d}v_\parallel \mathrm{d}\mu \ v_\parallel J_0(\lambda_s) F_{1,s}(\mathbf{x}, v_\parallel, \mu) \ . \tag{4.31}$$

Fourier transformation and normalization yields

$$k_{\perp\mathrm{N}}^2 \widehat{A}_{1\parallel\mathrm{N}} = 2\pi B_\mathrm{N} \beta_\mathrm{ref} \sum_s Z_s n_{\mathrm{R},s} v_{\mathrm{thR},s} \int \mathrm{d}v_{\parallel\mathrm{N}} \mathrm{d}\mu_\mathrm{N} \ v_{\parallel\mathrm{N}} J_0(k_\perp \rho_s) \widehat{F}_{1\mathrm{N},s} \ . \tag{4.32}$$

### 4.5.4 Cancellation Problem

Global Gyrokinetic simulations are suffering from numerical problems, mainly from the cancellation problem[3] examined in codes which uses the paticle-in-cell or the Eulerian methods[5]. This problem limits the electromagnetic investigations to extremely low $\beta$ parameters.[13] As in Chapter 3.3.2 discussed appears in the Source term [Eq. (3.39)] the time derivative of the parallel pertrubed vector potential $\partial_t \bar{A}_{1\parallel}$. This $A_{1\parallel}$-Term and the $\partial t F_1$ term in the gyrokinetic equation are computationally difficult to handle, as it is not immediately clear how to evaluate the terms using an simple Runge-Kutta scheme. To avoid further complications a modified distribution function $g$ gets introduced

$$g = F_1 + \frac{Zev_\parallel}{T}\bar{A}_{1\parallel}F_\mathrm{M} \ . \tag{4.33}$$

Substituting the modified distribution function $g$ into Equation (3.33) results in

$$\frac{\partial g}{\partial t} + \mathbf{v}_\chi \cdot \nabla g + (v_\parallel \mathbf{b}_0 + \mathbf{v}_\mathrm{D}) \cdot \nabla F_1 - \frac{\mathbf{b}_0}{m} \cdot (Ze\nabla\Phi_0 + \mu\nabla B_0 - mR\Omega^2\nabla R)\frac{\partial F_1}{\partial v_\parallel} = S \tag{4.34}$$

with the source term $S$ defined as

$$S = -(\mathbf{v}_\chi + \mathbf{v}_\mathrm{D}) \cdot \tilde{\nabla} F_\mathrm{M} - \frac{F_\mathrm{M}}{T}(v_\parallel \mathbf{b}_0 + \mathbf{v}_\mathrm{D}) \cdot (Ze\nabla\bar{\Phi} + \mu\nabla\bar{B}_{1\parallel}) \ . \tag{4.35}$$

This method is currently implemented in **GKW**[14]. The advantage of this substitition is clear, because now only one time derivative appears in the gyrokinetic equation. Due to the substitition the distrubution function $F_1$ in thge field equations has to be replaced by with the modified distribution $g$. For the equations of pertrubated electrostatic potential $\Phi_1$ and parallel magnetic field $B_{1\parallel}$ the replacement is trivial since the integral $\int \mathrm{d}v_\parallel v_\parallel = 0$ (due to symmetry) results in the elimination of the $A_{1\parallel}$-Term in both equation leaving the modified distribution $g$ in the integral. For the field equation for $A_{1\parallel}$ the substitition has a different effect. By replacing $F_1$ with $g$ the new normalized fourier transfromed field equation for $A_{1\parallel}$ is given by

$$\begin{aligned} &\left(k_{\perp\mathrm{N}}^2 + \beta_\mathrm{ref}\sum_s \frac{Z_s^2 n_{\mathrm{R},s}}{m_{\mathrm{R},s}}\Gamma_0(b_s)e^{-\mathcal{E}_{\mathrm{N},s}/T_{\mathrm{R},s}}\right)\widehat{A}_{1\parallel\mathrm{N}} = \\ &2\pi B_\mathrm{N}\beta_\mathrm{ref}\sum_s Z_s n_{\mathrm{R},s} v_{\mathrm{thR},s}\int \mathrm{d}v_{\parallel\mathrm{N}}\mathrm{d}\mu_\mathrm{N}\ v_{\parallel\mathrm{N}}J_0(k_\perp\rho_s)\widehat{g}_{\mathrm{N},s} \ . \end{aligned} \tag{4.36}$$

Comparing Eq. (4.32) and Eq. (4.36) one will notice the additional term in the brackets of Eq. (4.36). This term is the so-called *skin term*[12] and has no physical meaning and only appears because of the substitution of the distribution function. To understand the cancellation problem completely, one has to consider the "hidden" $A_{1\parallel}$ term in the

distrubution $g$. This $A_{1\parallel}$ term has to be cancelled exactly with the skin term. But due to the different numerical representation of the skin term (analytically) and the integral over the modified distribution function (numerically), the cancellation gets inexact and leads to the cancellation problem. The error of the cancellation scales with $\beta_{\mathrm{ref}}/k_{\perp\mathrm{N}}^2$, making simulations with hig plasma beta und small $k_\perp$ very challenging. To mitigate the cancellation problem the gamma function $\Gamma(b)$ gets also calculated with the same numerical scheme as the integral over the distrubution, but this approuch has to be performed carefully and could still lead to errors.

### 4.5.5 Faraday's Law - Inductive Electric Field $\boldsymbol{E_{1\parallel}}$

The goal of this Chapter is to handle the $\partial_t \bar{A}_{1\parallel}$ term with the consideration of electromagnetic fields and rework the Vlasov equation and fiels equations for **GKW** . This section follows the work of P.C. Crandall in his Disseration[4].

First the Vlasov equation gets written down in the $F_1$ framework with the source term [Eq. (3.33) & (3.39)] will get simplified into

$$\frac{\partial F_1}{\partial t} + \frac{Zev_\parallel}{T}\partial_t \bar{A}_{1\parallel} F_\mathrm{M} = \mathcal{V} \ , \tag{4.37}$$

where $\mathcal{V}$ represents all terms of the Vlasov Equation which excludes the time derivative of plasma induction $\partial_t \bar{A}_{1\parallel}$. The equation of the $\bar{A}_{1\parallel}$ is already astablished in Chapter 4.5.3 but for this derivation a recall will be made. The equation for $\bar{A}_{1\parallel}$ is given by

$$\nabla^2 A_{1\parallel} = -\mu_0 j_{1\parallel} = -\sum_s \frac{2\pi Z_s e \mu_0 B_0}{m_s} \int \mathrm{d}v_\parallel \mathrm{d}\mu \ \langle v_\parallel F_{1,s} \rangle \ . \tag{4.38}$$

Now the following formalism will be used

$$E_{1\parallel} = -\frac{\partial A_{1\parallel}}{\partial t} \ . \tag{4.39}$$

Taking the time derivative of Equation (4.38) results into the field equation for the induced electric field $E_{1\parallel}$ which can be expressed as

$$\nabla^2 E_{1\parallel} - \sum_s \frac{2\pi Z_s e \mu_0 B_0}{m_s} \int \mathrm{d}v_\parallel \mathrm{d}\mu \ \langle v_\parallel \frac{\partial F_{1,s}}{\partial t} \rangle = 0 \ . \tag{4.40}$$

In Equation (4.40) the time derivative of the gyrocenter distrubution function has to be further simplified for that the gyrokinetic equation shall be rewritten as

$$\frac{\partial F_1}{\partial t} = \mathcal{V} + \frac{Zev_\parallel}{T} \bar{E}_{1\parallel} F_\mathrm{M} \ . \tag{4.41}$$

Plugging Equation (4.41) into Equation (4.40), one can derive the equation for the inductive electric field

$$\begin{aligned} &\left( \nabla^2 - \sum_s \frac{2\pi (Z_s e)^2 \mu_0 B_0}{T_s m_s} \int \mathrm{d}v_\parallel \mathrm{d}\mu \ \mathcal{G}^\dagger v_\parallel^2 F_{\mathrm{M}s} \mathcal{G} \right) E_{1\parallel} = \\ &\sum_s \frac{2\pi Z_s e \mu_0 B_0}{m_s} \int \mathrm{d}v_\parallel \mathrm{d}\mu \ \mathcal{G}^\dagger \left\{ v_\parallel \mathcal{V}_s \right\} = \mu_0 \frac{\partial j_{1\parallel}}{\partial t} \ , \end{aligned} \tag{4.42}$$

although the relation of $\bar{E}_{1\parallel} = \mathcal{G}\left\{E_{1\parallel}\right\}$ and the definition of $\mathcal{G}^\dagger$ was used to simplyfied the integral on the right-hand side. To complete the derivation of this section the delta-*f*

Vlasov equation will be recalled with the inductive filed $E_{1\parallel}$ in the source term. The delta-$f$ Vlasov equation is given by

$$\frac{\partial F_1}{\partial t} + \dot{\mathbf{X}} \cdot \nabla F_1 - \frac{\mathbf{b}_0}{m} \cdot \left( Ze\nabla\Phi_0 + \mu\nabla B_0 - mR\Omega^2\nabla R \right) \cdot \frac{\partial F_1}{\partial v_\parallel} = S \ , \tag{4.43}$$

with the source term

$$\begin{aligned} S = &-(\mathbf{v}_\chi + \mathbf{v}_\mathrm{D}) \cdot \tilde{\nabla} F_\mathrm{M} + \frac{Zev_\parallel}{T} \bar{E}_{1\parallel} F_\mathrm{M} \\ &- \frac{F_\mathrm{M}}{T} (v_\parallel \mathbf{b}_0 + \mathbf{v}_\mathrm{D} + \mathbf{v}_{\bar{B}_{1\perp}}) \cdot (Ze\nabla\bar{\Phi} + \mu\nabla\bar{B}_{1\parallel}) \ . \end{aligned} \tag{4.44}$$

Using the new definition of the gyrooperator into Equation (4.40), one can derive the equation for the included electric field

$$\begin{aligned} &\left( \nabla^2 - \sum_s \frac{2\pi (Z_s e)^2 \mu_0 B_0}{T_s m_s} \int \mathrm{d}v_\parallel \mathrm{d}\mu \ v_\parallel^2 J_0^2(\lambda_s) F_{\mathrm{M}s} \right) E_{1\parallel} = \\ &\sum_s \frac{2\pi Z_s e \mu_0 B_0}{m_s} \int \mathrm{d}v_\parallel \mathrm{d}\mu \ v_\parallel J_0(\lambda_s) \mathcal{V}_s = \mu_0 \frac{\partial j_{1\parallel}}{\partial t} \ , \end{aligned} \tag{4.45}$$

although the relation of $\bar{E}_{1\parallel} = \mathcal{G}\left\{E_{1\parallel}\right\} = J_0(\lambda) E_{1\parallel}$ was used to simplyfied the integral on the right-hand side. The integral itself can be more simplified with performing the integral over $v_\parallel$ and $\mu$

$$\begin{aligned} I &= \frac{2\pi (Ze)^2 \mu_0 B_0}{Tm} \int \mathrm{d}v_\parallel \mathrm{d}\mu \ v_\parallel^2 J_0^2(\lambda) F_\mathrm{M} \\ &= \frac{2\pi (Ze)^2 \mu_0 B_0}{Tm} e^{-\mathcal{E}/T} \underbrace{\int \mathrm{d}v_\parallel \ v_\parallel^2 F_\mathrm{M}(v_\parallel)}_{n_{R_0}/2\pi} \underbrace{\int \mathrm{d}\mu \ J_0^2(\lambda) F_\mathrm{M}(\mu)}_{T/B_0 \ \Gamma_0(b)} \\ &= \frac{(Ze)^2 \mu_0 n_{R_0}}{m} \Gamma_0(b) e^{-\mathcal{E}/T} \ , \end{aligned} \tag{4.46}$$

where the seperation of the Maxwellian was used [Eq. (3.37)]. Finally, the field equation for the induced electric field can be written as

$$\begin{aligned} &\left( \nabla^2 - \sum_s \frac{Z_s^2 e^2 \mu_0 n_{R_0,s}}{m_s} \Gamma_0(b_s) e^{-\mathcal{E}_s/T_s} \right) E_{1\parallel} = \\ &\sum_s \frac{2\pi Z_s e \mu_0 B_0}{m_s} \int \mathrm{d}v_\parallel \mathrm{d}\mu \ v_\parallel J_0(\lambda_s) \mathcal{V}_s = \mu_0 \frac{\partial j_{1\parallel}}{\partial t} \ . \end{aligned} \tag{4.47}$$

After performing the Fourier transform and normalize Equation (4.47) the final field equation for the inductive electric field is given by

$$\begin{aligned} &\left( k_{\perp\mathrm{N}}^2 + \beta_\mathrm{ref} \sum_s \frac{Z_s^2 n_{\mathrm{R},s}}{m_{\mathrm{R},s}} \Gamma_0(b_s) e^{-\mathcal{E}_{\mathrm{N},s}/T_{\mathrm{R},s}} \right) \widehat{E}_{1\parallel\mathrm{N}} = \\ &- 2\pi B_\mathrm{N} \beta_\mathrm{ref} \sum_s Z_s n_{\mathrm{R},s} v_{\mathrm{thR},s} \int \mathrm{d}v_{\parallel\mathrm{N}} \mathrm{d}\mu_\mathrm{N} \ v_{\parallel\mathrm{N}} J_0(k_\perp \rho_s) \widehat{\mathcal{V}}_{\mathrm{N},s} \ . \end{aligned} \tag{4.48}$$

CHAPTER

# Plasma Induction in Local Gyrokinetic Simulations

5

## 5.1 Gyrokinetic Workshop (GKW )

## 5.2 Implementation

### 5.2.1 Improvements

At the beginning, it is necessary to talk about the applied code improvements which where done to ensure a valid implementation of the Faraday Law into **GKW** .

(1) In diagnostics part of **GKW** serveral subroutines and functions relies on the definition of the variable `requirements` from the module `diagnostics.f90`. The variable `requirements` is a matrix which communticates which type of data or ghost cell needs to be provided to the diagnostic. In the previous implementation the number of columns were hard coded the field identifier for the gyroaveraged parallel magnetic field $\bar{B}_{1\parallel}$ with `BPAR_GA_FIELD`. This type of problem was found on multiple occasions throughout the code most noteable in `dist.f90` with `derivs_in_lin_terms` and the token array in `diagnos_generic.f90`. Furthermore, it was found that in the code more inconvienece sturcutures were established. For example slicing the `requirements` matrix was performend by `PHI_FIELD:BPAR_FIELD` and `PHI_GA_FIELD:BPAR_GA_FIELD`, the start of the tokens for moments with `BPAR_GA_FIELD` and the definition for the distrubution function to the number 4. To prevent any errors with future modifications, for example an additional new field, new variabels and scheme gets introduced in `global.f90` as

- `MIN_FIELD` as the smallest number of field identifier,
- `MIN_GA_FIELD` as the smallest number of gyroaverages field identifier
- `MAX_FIELD` as the greatest number of field identifier,
- `MAX_GA_FIELD` as the greatest number of gyroaverages field identifier,
- `DISTRIBUTION` should always have the greatest number and
- `MAX_IDX_FIELD` is the greatest number, i.e. `DISTRIBUTION`.

These changes allowed to the implementation `EPAR_FIELD` and `EPAR_GA_FIELD` as

- `EPAR_FIELD = 4`,
- `EPAR_GA_FIELD = 8`

as well as a new scheme for slicing gets introduced

- `PHI_FIELD:BPAR_FIELD` replaced by `MIN_FIELD:MAX_FIELD`,
- `PHI_GA_FIELD:BPAR_GA_FIELD` replaced by `MIN_GA_FIELD:MAX_GA_FIELD`.

Note that, with the variables the slicing gets performend from `PHI_FIELD` to `EPAR_FIELD` and `PHI_GA_FIELD` to `EPAR_GA_FIELD`, since the field indentifier for inductive electric field $E_{1\parallel}$ is the greatest number in both cases. The field identifier for the distribution functionen $F_1$ changed to the number 9 and the size of the arrays or matrix is defined by `MAX_IDX_FIELD`. It is advicable to make sure that the

field identifier for the distrubution function is always the greatest number. Further changes were performed in the whole code to ensure the new scheme. The changed code sequence in `global.f90` is listed below

```
!------------------------------------------------------------------
!> Please note following notation to prevent errors in diagnostics,
!> check input (through requirements) and creation of ghost cells.
!>
!> - MIN_FIELD = smallest number of field identifier
!> - MIN_GA_FIELD = smallest number of gyroaverages field identifier
!> - MAX_FIELD = greatest number of field identifier
!> - MAX_GA_FIELD = greatest number of gyroaverages field identifier
!>
!> - DISTRIBUTION should always have the greatest number
!>
!> - MAX_IDX_FIELD = the greatest number, i.e. DISTRIBUTION
!------------------------------------------------------------------
integer, parameter, public :: PHI_FIELD  = 1, APAR_FIELD = 2
integer, parameter, public :: BPAR_FIELD = 3, EPAR_FIELD = 4
integer, parameter, public :: PHI_GA_FIELD  = 5, APAR_GA_FIELD = 6
integer, parameter, public :: BPAR_GA_FIELD = 7, EPAR_GA_FIELD = 8
integer, parameter, public :: DISTRIBUTION = 9
integer, parameter, public :: EVERY_FIELD = 0

integer, parameter, public :: MIN_FIELD     = PHI_FIELD
integer, parameter, public :: MAX_FIELD     = EPAR_FIELD
integer, parameter, public :: MIN_GA_FIELD  = PHI_GA_FIELD
integer, parameter, public :: MAX_GA_FIELD  = EPAR_GA_FIELD
integer, parameter, public :: MAX_IDX_FIELD = DISTRIBUTION
```

(2) Since the calculation of $E_{1\parallel}$ needs the right-hand side of the Vlasov equation $\mathcal{V}$ and the regular fields perform the calculation with the distrubution function *df* a seperation between additional and regular field equations were done. For that purpose new the variables gets introduced in `dist.f90` that follows the existing notation

- `nregular_fields_start` as the start of the solutions of the regular fields, i.e. $\Phi$, $A_{1\parallel}$ and $B_{1\parallel}$, in `fdisi`,
- `nadditional_fields_start` as the start of the solutions of the additional fields, i.e. $E_{1\parallel}$, in `fdisi`,
- `nadditional_fields_end` as the end of the solutions of the regular fields in `fdisi`.

Here, `nregular_fields_start` replaces the variable `n_phi_start` to improve the code to a more general naming scheme. Note that, the declaration of the new variables have a specific place in the code and should not be changed. So, if someone wants to add a new regular field the definition of the number of elements in `fdisi` and ghost cells should be put above the declaration from `nregular_fields_start` and `nregular_fields_end` the same goes for additonal fields.

(3) The size of the field matrix `poisson_int` and `mat_field_diag` in the module `matdat.f90` was implemented to big with the size of `ntot` which is the number grid points for the whole array `fdisi`. To add a more natrual way to define the size of the regular field matrices the new variable `nelem_regular_fields` gets defined as `nelem_regular_fields = nf *(1 * number_of_fields)` in `dist.f90`. Here, `nf = nsp*nx*nmu*nvpar*nmod` stands for the number of grid points for the distribution function $F_1$ and `number_of_fields` is an integer which gets incremented by one for every activated field calculation. In general, `nelem_regular_fields` is always lesser than `ntot` which could improve the runtime of the code, because allocating the field matixes does take less time than before. The declaration of `nelem_regular_fields` is in the same code block as `nregular_fields_start` and `nregular_fields_end` and should not be changed, since it relies heavily on the parameter `number_of_fields`.

(4) In the subroutine `calculate_fields` in `fields.f90` the division of the diagonal parts of the regular fields was performed by a loop starting at `nregular_fields_start` and ends at the size of `mat_field_diag`. Since it was very unintuitiv to start a loop not at one further investigations were done and it was found that in `linear_terms.f90` a unity block of the size of `nf` was added in the front of the first element of `mat_field_diag`. This performed action was removed and teh loop in `calculate_fields` adjust to loop from the first element to the last element of `mat_field_diag`.

(5) The subroutine `g2f_correct` from the module `linear_terms` gets renamed to `apar_correct`, which suits the new established naming scheme and purpose for the subroutine.

(6) Overall at multiple occasions the code syntax got corrected as well as some minor mistakes.

### 5.2.2 $E_{1\parallel}$ Field Equation

Since the code is capable of parallization the inserted code is written to use the OpenMPI libary. This will from now on uncomment. Further subtile changes or import statements will be uncommented since most of them are just following the eastablished stucture for $A_{1\parallel}$ and add them for $E_{1\parallel}$ into the code as well. The reader is referred to the branch in bibucket[9] for more in depth documentation on the process and implementation.

#### Feature Switch

For the calculation for $E_{1\parallel}$ one has to add a switch into `control.f90` which relates to the parameter `nlepar`. By default, `nlepar` is set to `.false.`. Additionally, `nlapar` will also be set `.true.`, because $E_{1\parallel} = \partial_t A_{1\parallel}$. All upcoming changes in the code can only be accessed if `nlepar` is set to `.true.` which gets implemented with an if statement.

#### Identifiers `iepar` and `iepar_ga`

In the next step the identifieres for the $E_{1\parallel}$ and $\bar{E}_{1\parallel}$ will be defined in `dist.f90`. These identifieres makes it possible to access only $E_{1\parallel}$ and $\bar{E}_{1\parallel}$ in teh solution `fdisi` with the use of the index function from the module `index_function.f90`. The definition of the identifieres follows the already established scheme with the name `iepar` and `iepar_ga` although

- `iepar = 4 + IS_3D_FIELD = 12` with `IS_3D_FIELD = 2**3 = 8` and
- `iepar_ga = 4 + IS_GYROAVG_FIELD = 36` with `IS_GYROAVG_FIELD = 2**5 = 32`.

It was checked, if the new indentifiers are not used from the existing implementation.

#### Definition of Grid Points and Ghost Cells

To continue the implementation, the grid points of $E_{1\parallel}$ gets defined as well as the ghost cells of $E_{1\parallel}$.

```
! the fields, EXCLUDING gyroavg fields and EXCLUDING the
  ↪ collisionop-related fields
nregular_fields_end = nf + nfields
! total number of elements in mat_possion and mat_field_diag
nelem_regular_fields = nf * (1 + number_of_fields)
! N.B. no more regular fields are allowed after here.
```

```
! if the inductive electric field is kept increase the size
if (nlepar) then
  number_of_fields = number_of_fields + 1
  n_epar           = nf + nfields
  nelem_epar       = nx*ns*nmod
  nfields          = nfields + nelem_epar
```

Here, `number_of_fields` refers to the total number of fields that gets calculated, `n_epar` to the start of the grid points for $E_{1\|}$ in `fdisi`, `nelem_epar` for the amount of grid points and `nfields` for all grid points for the fields calculation, i.e. additonal and regular fields. Additionally, the maximum number of grid points for $E_{1\|}$ (`nf`) gets added to the total number of grid points `ntot` with `ntot = ntot + nf`, where `nf` equals the number of grid points for the distribution function $F_1$.

It is necessary to mentioned that the implementation of the grid points for $E_{1\|}$ results in an compliation error of **GKW** . The error is strongly connected to the variable `field_id` which is used to create an quick look up array for the fields in the function `get_field_index_lookup_array` in `diagnos_growth_freq` and `diagnos_timetrace` as well as in a code section in the subroutine `normalise_init` in the module `normalise`. The main problem in the function `get_field_index_lookup_array` is, that the size of the array `field_id` gets allocated with the variable `number_of_fields` form module `dist`. The incremtation of `number_of_fields` by $E_{1\|}$ results in an **GKW** error called "bad identifier". Adding $E_{1\|}$ into the function solves the issue. In the subroutine `normalise_init` the code for $E_{1\|}$ and $\bar{E}_{1\|}$ has to be added as well as the allocated size of `field_id` increased by two. At the end in the subroutine `calc_phase` from the module `diagnos_growth_freq` the size of the array `field_id` has also be incremented by one to prevent any bad identifiers.

### Calculation of $E_{1\parallel}$

Before the implementation for the calculation of $E_{1\parallel}$ gets discussed it is necessary to talk about the scheme of the calculation. As stated in Equation (4.48) is the right-hand side of the Vlasov equation $\mathcal{V}$ necessary for the calculation of $E_{1\parallel}$. Now, if one takes a closer look at Equations (4.33) and (4.37) it can be derived that

$$\frac{\partial g}{\partial t} = \mathcal{V} \ , \tag{5.1}$$

where $g$ is the modified distribution. Since **GKW** has already implemented $\partial_t g$ as `rhs` (right-hand side) and the Vlasov equation with the modified distribution function [Eq (4.34)] has only one additional term containing $g$, which is nonlinear, i.e. ignored in linear cases, `rhs` will be used as the right-hand side of the Vlasov equation in the calculation of $E_{1\parallel}$. In the next step the numerical scheme for every Runge Kutta step ($i \to i+1$) has to be considered. Figure 5.1 gives an illustration of the scheme.

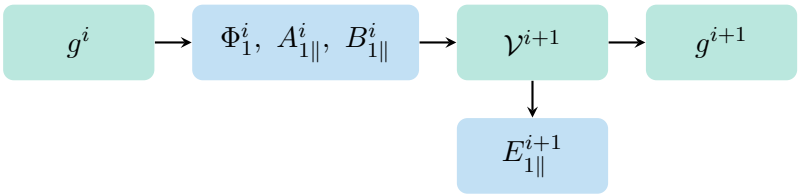


Figure 5.1: Numerical scheme used to calculate the induced eletric field $E_{1\parallel}$ in **GKW** .

As visible, the order of calculations is important in the numerical scheme, i.e. first calculate the right-hand side of the Vlasov equation $\mathcal{V}$ and afterwards the induced electric field $E_{1\parallel}$. To achieve this structure the calculation of $E_{1\parallel}$ gets performed in `calculate_rhs` from the module `exp_integration`. For that, the following code lines get added in `calculate_rhs`

```
if (nlepar) then
  if(perf_measure) then
    call perfswitch('Calc Additonal Fields',2)
    perffields=.true.
  end if

  ! Calculate the additional fields with rhs, i.e. epar,
  ! from rhs into fdis (fdis = mat * rhs) and apply the rhs
  ! correction with rhs = rhs + A * ga{epar}
  ! Note that rhs gets saved as rhs * deltatime which gets
  ! corrected in calculate_additional_fields
  if (spectral_radius) then
    call calculate_additional_fields(fdis, rhs, deltatime)
  endif

  if (perf_measure) then
```

```
      call perfswitch('Copy fdis vector to tmp',2)
      perffields=.false.
    end if
```

To ensure that the right Runge Kutta step for the calculatation of $E_{1\parallel}$ is used, the following lines have to be adjusted in the subroutine `advance_large_step_explicit` in the same module.

```
  ! at the end of the timestep, make the electromagnetic field
  ! consistent with the distribution function
  if (spectral_radius) then
    ! Do not change the order because of the calculation scheme
    ! f_i -> Phi_i, Apar_i, Bpar_i -> RHS_i+1 -> Epar_i+1 -> f_i+1
    ! Since calculate_fields gets called in calculate_rhs it does not
    ! have to be called before.
    if (nlepar) then
      call calculate_rhs(fdisi, rhsk(:,1))
    else
      call calculate_fields(fdisi)
    endif
  else
```

Note that, before the implementation of $E_{1\parallel}$ feature, `calculate_fields` gets called for local simulations, but since the calculation of $E_{1\parallel}$ requires the calculation of the right-hand side $\mathcal{V}$, which calculates the regular fields already in the subroutine `calculate_rhs`, the call for `calculate_fields` can be neglected if $E_{1\parallel}$ gets calculated.

The calculation of $E_{1\parallel}$ itself gets performed by `calculate_additonal_fields` from the module `fields`. The subroutine is listed below

```
!------------------------------------------------------------------------
!> This routine calculates the integrated quantities of the perturbed
!> distribution function with the use of the right hand side. It is
!> used to calculate the induced electric field.
!>
!> It is an optimized routine, meaning that explicit assumptions are
!> made on the the memory layout of the code.
!>
!> calls MPI_ALL_REDUCE to sum and distribute the integrals to all
!> processors.
!>
!> Note that, rhs gets saved as rhs * dtim * c1 in calculate_rhs which
!> has to be corrected with rhs/(dtim*c1). For that, the argument
!> DTIM = dtim*c1 = deltatime should be used.
!------------------------------------------------------------------------
subroutine calculate_additional_fields(fdis, rhs, DTIM, DPART)  ! OPTIMISED
    ↪ routine

  use dist,           only : nsolc
  use dist,           only : nadditional_fields_start, nadditional_fields_end
  use matdat,         only : mat_add_field_int, mat_add_field_diag
  use control,        only : nlepar, nlapar
  use general,        only : gkw_warn
```

```
use mpiinterface,   only : number_of_processors, mpiallreduce_sum_inplace
use mpicomms,       only : COMM_S_EQ
use components,     only : tearingmode
use perform,        only : perfon, perfoff, perffields, perf_measure
use perform,        only : perfswitch
use matrix_format,  only : usmv

complex, optional, intent(inout) :: rhs(nsolc)
complex, intent(inout) :: fdis(nsolc)

integer :: i
integer :: ierr

! small timestep to divide rhs * dtime to correct to only rhs
complex, intent(in) :: DTIM
real, optional, intent(in) :: DPART

! warning #1 here an assumption of the postion of phi in
! the solution is made. I.e. the index function is not
! used. This is of course faster.
!APS: This could be replaced with another appropriate integer denoting the
!APS: index of the first field element.

!Initialise to zero (required if fields are not solved: tearingmodes,
  ↪ tracers)
!$omp parallel do schedule(static)
zero : do i = nadditional_fields_start, nadditional_fields_end
  fdis(i) = (0.E0,0.E0)
end do zero
!$omp end parallel do

! no point in calculating the potential if it is to
! be zero. (important also for the testcases that do not use phi)
if ((.not. nlepar .and. .not. nlapar)) then
  return
end if

if (perffields .and. perf_measure) then
  call perfon('add fields - int mat multiply',2)
end if

! first calculate the contribution of rhs
call usmv(cmplx(1.0,0.0),mat_add_field_int,rhs/DTIM,fdis,ierr)

if (perffields .and. perf_measure) call perfswitch('add fields - MPI
  ↪ allreduce',2)

if (number_of_processors > 1) then
  ! finish the species sum and the velspace integral
  call
  ↪ mpiallreduce_sum_inplace(fdis(nadditional_fields_start:nadditional_fields_end),&
     nadditional_fields_end-nadditional_fields_start+1,COMM=COMM_S_EQ)
end if
```

```
  !
  if (perffields .and. perf_measure) call perfswitch('add fields - n4 renorm
    ↪ diag',2)

  ! Then divide by A: division by fields diagonal part, all elements
  ! are independent. Since we know that mat_add_field_diag has a NO unity
  ! block in the distribution part of the matrix, one has to start form i =
    ↪ 1.
  normalise : do i = 1, mat_add_field_diag%nmat
    fdis(mat_add_field_diag%ii(i)) =
    ↪ fdis(mat_add_field_diag%ii(i))*mat_add_field_diag%mat(i)
  end do normalise

  tearingmod : if(tearingmode) then
    call gkw_warn('Tearing modes are not implemented for additional fields
    ↪ yet')
  end if tearingmod

  if (perffields .and. perf_measure)  call perfoff(2)

end subroutine calculate_additional_fields
```

This subroutine has the same structure as `calculate_fields` with two major differences. No tearing modes are implemented yet and if tearing modes are activated, a warning gets printed to the console. `rhs` and `DTIM` as additonal argument for the subroutine. The use of `rhs` was already discussed at the beginning of this section but the variable `rhs`, which gets communticated in `calculate_rhs` is not already the right right-hand side needed for the calculation of $E_{1\parallel}$. `rhs` is a product of `rhs` and the time step `deltatime`. This is due to the Runge Kutta scheme for the calculatation of the distribution function $g$. To ensure that the "pure" right-hand side $\mathcal{V}$ will be used for $E_{1\parallel}$ the argument `DTIM` in `calculate_additonal_fields` is used to divide `rhs` by `DTIM`, which is `deltatime` from `calculate_rhs`.

In **GKW** the calculation of the $E_{1\parallel}$ field gets performed in two steps:

(1) Matrix vector multiplication of the matrix containing the integral part of $E_{1\parallel}$ with the "pure" right-hand side array `rhs/DTIM`
`fdisi = mat_add_field_int * (rhs / DTIM)`

(2) Division of the matrix containing the diagonal part of $E_{1\parallel}$
`fdisi = fdisi / mat_add_field_diag`.

Both operations gets saved in the solution array `fdisi`. The integral part (`faraday_int`) and the diagonal part (`faraday_dia`) gets extracted from Equation (4.48) and defined as

$$\begin{aligned} \texttt{faraday\_int} &= -2\pi B_{\mathrm{N}} \beta_{\mathrm{ref}} \sum_s Z_s n_{\mathrm{R},s} v_{\mathrm{thR},s} \int \mathrm{d}v_{\parallel \mathrm{N}} \mathrm{d}\mu_{\mathrm{N}}\ v_{\parallel \mathrm{N}} J_0(k_{\perp} \rho_s) \\ \texttt{faraday\_dia} &= \left( k_{\perp \mathrm{N}}^2 + \beta_{\mathrm{ref}} \sum_s \frac{Z_s^2 n_{\mathrm{R},s}}{m_{\mathrm{R},s}} \Gamma_0(b_s) e^{-\mathcal{E}_{\mathrm{N},s}/T_{\mathrm{R},s}} \right) . \end{aligned} \tag{5.2}$$

`faraday_int` and `faraday_dia` both are defined in the module `linear_terms` in two seperate subroutions given below

```
  end if

end subroutine ampere_bpar_int

!------------------------------------------------------------------------------
!> Adds the part of the Faraday's law that is related with
!> the integral over the right hand side of the vlasov equation.
!------------------------------------------------------------------------------
subroutine faraday_int

  use structures,     only : matrix_element
  use control,        only : nlepar, spectral_radius
  use grid,           only : nx,ns,nmu,nvpar,nsp,nmod
  use components,     only : de, signz, vthrat, veta
  use matdat,         only : add_element, set_indx
  use geom,           only : bn
  use velocitygrid,   only : vpgr, intvp, intmu
  use dist,           only : ifdis, iepar
  use functions,      only : besselj0_gkw

  real                   :: bes
  integer                :: ix, i, j, k, is, imod, ierr
  type (matrix_element) :: elem

  ! non spectral case is done elsewhere (in gyro_average)
  if (.not. spectral_radius) return

  ! Indentifier for the term
  elem%term = 'faraday_int'

  ! Type of iih and jjh
  elem%itype = iepar
  elem%itloc = ifdis
  elem%ideriv = 0

  if (.not. nlepar) return

  do imod = 1, nmod

    if (all(apply_on_imod == 0)) then
      if(.not. lfaraday) cycle
    else
      if (any(apply_on_imod == imod)) then
        if(.not. lfaraday) cycle
      else
        if(.not.linear_term_switch_default) cycle
      endif
    endif

    do ix = 1, nx ; do i = 1, ns ; do j = 1, nmu ; do k = 1, nvpar ; do is =
    ↪ 1, nsp
```

```
      call set_indx(elem,imod,ix,i,j,k,is)

      ! Bessel function for gyro-average
      bes = besselj0_gkw(imod,ix,i,j,is)

      elem%val = -signz(is)*de(ix,is)*veta(ix)*intvp(i,j,k,is)*intmu(j)
    ↪ &
```

```
        ! later because multiplication is faster than division.
        elem%val = -1.0/(mat_elem + dum)
      endif

      call add_element(elem,ierr)

    end do ; end do

  end do

end subroutine ampere_dia

!---------------------------------------------------------------------------
!> Add the diagonal part of Faraday's law
!---------------------------------------------------------------------------
subroutine faraday_dia

  use structures,     only : matrix_element
  use control,        only : nlepar, spectral_radius
  use grid,           only : nx,ns,nsp,nmod,nmu,nvpar
  use mpicomms,       only : COMM_S_EQ
  use dist,           only : fmaxwl, iepar
  use components,     only : de, signz, mas, veta
  use matdat,         only : add_element, set_indx
  use geom,           only : bn
  use mode,           only : krloc
  use rotation,       only : cfen
  use velocitygrid,   only : intvp, intmu, vpgr
  use functions,      only : gamma_gkw, besselj0_gkw
  use mpiinterface,   only : mpiallreduce_sum_inplace

  real    :: gamma, gamma_num, b, dum
  integer :: imod, ix, i, j, k, is, idum, ierr
  complex :: mat_elem
  type (matrix_element) :: elem

  ! non spectral case is done elsewhere (in gyro_average - integral term)
  if (.not. spectral_radius) return

  if (.not. nlepar) return

  ! indentifier of the term
  elem%term = 'faraday_dia'
  elem%itype = iepar
  elem%itloc = iepar
```

```
elem%ideriv = 0

! set the dummy
idum = 0

do imod = 1, nmod

  if (all(apply_on_imod == 0)) then
    if(.not. lfaraday) cycle
  else
    if (any(apply_on_imod == imod)) then
      if(.not. lfaraday) cycle
    else
      if(.not.linear_term_switch_default) cycle
    endif
  endif

  do ix = 1, nx ; do i = 1, ns

    ! reference Epar
    call set_indx(elem,imod,ix,i,idum,idum,idum)

    ! The nabla^2 term
    mat_elem =  - krloc(imod,ix,i)**2

    ! calculate the Maxwell correction
    dum = 0.
    do is = 1, nsp

      ! The gamma function of the species
      gamma = gamma_gkw(imod,ix,i,is)*exp(-cfen(i,is))

      ! numerical calculation of the gamma function
      !(includes the strong rotation correction implictly in the
↪ maxwellian)
      gamma_num = 0.
      do j = 1, nmu ; do k = 1, nvpar
        b = besselj0_gkw(imod,ix,i,j,is)
        gamma_num = gamma_num +
↪ 2.E0*bn(ix,i)*intmu(j)*intvp(i,j,k,is)*b**2* &
                & vpgr(i,j,k,is)**2*fmaxwl(ix,i,j,k,is)
        ! The implementation below was used until Feb 2023
        ! It is a bit more stable numerically but inaccurate at default
↪ vpmax
        ! Leads to large errors at high beta and low kthrho
        ! gamma_num = gamma_num +
↪ bn(ix,i)*intmu(j)*intvp(i,j,k,is)*b**2*fmaxwl(ix,i,j,k,is)
      end do ; end do

      dum = dum - veta(ix)*signz(is)**2*de(ix,is)*gamma_num / mas(is)

    end do !nsp
```

Note that, the $2\pi$ factor in `faraday_int` is already included in the array `intmu`[15] and will

be ignored. Additionally, in `faraday_dia` a new calculation for the $\Gamma_0(b)$ [Eq (4.14)] was introduced from Yann Camenen in February 2023. The integral part will get added to the matrix `mat_add_field_int` and the diagonal part in `mat_add_field_diag`. Both matrices are defined in `matdat`. The size of the matrices gets defined with `nelem_additional_fields` in `dist` with the same method as `nelem_regular_fields`. It is important to mention, that the declaration has to be after the definition of grid points and ghost cells for the additional fields. Also, during the optimizition of the number of elements for `mat_add_field_int` and `mat_add_field_diag` it was found that the `nelem_additional_fields` can not be further reduced. It seems like the field matrices for the additional fields has to account the number of elements for regular field matrices as well. To investigate the matrices, they got added to the diagnostic module `diagnos_matrix` which handles the output.

### Diagnostic for $E_{1\parallel}$

To extract $E_{1\parallel}$ from `fdisi` the subroutine `get_epar` in `dist.f90` is needed and is given in greater detail below

```
      ghost_s = ghost_points_s
      ghost_x = ghost_points_x
    end if
    do i = 1-ghost_s, ns+ghost_s
      do ix = 1-ghost_x, nx+ghost_x
        do imod = 1, nmod
          bparc(imod,ix,i) = fdis(indx(ibpar,imod,ix,i))
        end do
      end do
    end do
  else
    ! bpar is not solved for and therefore set to zero
    bparc = (0.E0,0.E0)
  end if

end subroutine get_bpar

!+++++++++++++++++++++++++++++++++++++++++++++++++++++++++++++++++++++++++++++++
!> This routine copies the potential from the distribution into the the eparc
!> array. If nlepar = .false. eparc is set to zero
!-------------------------------------------------------------------------------
subroutine get_epar(fdis,eparc)
  use general, only : gkw_abort
  use control, only : nlepar
  use grid, only : nmod, nx, ns
  use index_function, only : indx
  complex, dimension(:), intent(inout) :: fdis
  complex, dimension(nmod,1-ghost_points_x:nx+ghost_points_x,&
     & 1-ghost_points_s:ns+ghost_points_s), intent(out) :: eparc
  integer :: ix, i, imod, ghost_s, ghost_x

  if (first_call) then
```

```
    call gkw_abort('get_epar: you can not call this before dist_init')
  end if

  if (nlepar) then

    ! copy epar
    if(size(fdis) == nsolc) then
```

In general the given subroutine checks if any parallization was done and copies all real and complex entries of $E_{1\parallel}$ into the argument `eparc` by looping over all grid points for $s$, $\psi$ and $\zeta$ coordinate. If `nlepar` is set to `.false.`, a zero data set will be return.

The subroutine `get_epar` gets called in `diagnostic` in the subroutine `fill_buffer` where the new defined field identifier `EPAR_FIELD` form module `global` is used.

```
  if (nlepar) then
   if(requirements(EPAR_FIELD,X_GHOSTCELLS) .or. &
      & requirements(EPAR_FIELD,S_GHOSTCELLS)) then
     call get_epar(fdis_tmp,epar)
   else if(requirements(EPAR_FIELD,LOCAL_DATA)) then
     call get_epar(fdisi,epar)
   end if
  end if
```

Here, the calculated values for $E_{1\parallel}$ gets copied from `fdisi` (or `fdis_tmp` for parallization) to the variable `epar` from the module `dist`. In **GKW** , each diagnostics computes and outputs a distinct physical quantity.[15]. In `diagnos_mode_struct` the code gets adapted for the implementation of $E_{1\parallel}$ and the new field identifier `EPAR_FIELD` by increasing the size of the arrays `mode_struct_lus`, `mode_struct_ids`, `mode_struct_names`, `local_write` and `global_write` by one element. It is worth mentioning that from now on the variabels `epar` and `eperp` are renamed to `ene_par` and `ene_perp`. After loading the data for $E_{1\parallel}$ from the variable `epar` in a loop for each species $N_s$, grid points in binormal direction $N_{\mathrm{mod}}$, radial direction $N_x$ and in field direction $N_s$ into the variable `epad`. Then, `epad` gets normalised by rotating relative to the maximum electrostatic potential $\Phi_1$ in the complex plane for each mode is $1 + 0i$ and saved in parallel data structure. For that, the end of the loop with variable `il` will be increased from 8 to 9 and the parallel data structure got adjusted for two additional columns for $E_{1\parallel}$, i.e. for real and imaginary values. Note that if `nlepar` is set to `.false.` the variable `epad` returns an zero array. Due to this behaviour the testcases

- `adiabat_collisions_momcon_ap`,
- `chease_cf_modebox`,
- `collisions_please_dont_break_me` and
- `zonal_flow_sixth_order_FD`

have to adjusted to contain the two zero columns from $E_{1\parallel}$ in the file `parallel.dat`

### Benchmark of $E_{1\parallel}$ Field Equation - Linear $\beta$ Scan

To benchmark the implementation of Faraday's law with $E_{1\parallel}$ multiple linear simulations for different plasma beta $\beta$ gets performed. The goal is to extract the linear growth rate $\gamma$ and frequency $\omega$ to compare the result for $E_{1\parallel}$ with $A_{1\parallel}$. General a given quantity saved in `parallel.dat` gets saved in two columns containing real and imaginary values. The rows are sorted by the species $N_{\mathrm{sp}}$, bidnormal gird points $N_{\mathrm{mod}}$, radial grid points $N_x$ and grid points along the field line $N_s$ and therefore $N_{\mathrm{sp}}N_{\mathrm{mod}}N_xN_s$ rows. Data stored in `parallel.dat` is defined as

$$\widehat{L}(s,t) = \exp(\gamma t + i\omega t)\widehat{L}(s) \ , \tag{5.3}$$

where $\widehat{L}(s,t)$ is the calculated data and $\widehat{L}(s)$ is the stored values.[15] Note that, $\widehat{L}(s,t)$ and $\widehat{L}(s)$ are complex. With Equation (5.3) one can derive the relation between $\widehat{E}_{1\parallel}$ and $\widehat{A}_{1\parallel}$ with Faraday's law [Eq. (4.39)] as

$$\begin{aligned}
\widehat{E}_{1\parallel}(s,t) &= -\partial_t \widehat{A}_{1\parallel}(s,t) \\
\exp(\gamma t + i\omega t)\widehat{E}_{1\parallel}(s) &= -\partial_t \left[\exp(\gamma t + i\omega t)\widehat{A}_{1\parallel}(s)\right] \\
\widehat{E}_{1\parallel}(s) &= -(\gamma + i\omega)\widehat{A}_{1\parallel}(s) \\
\widehat{E}^{\mathrm{R}}_{1\parallel}(s) + i\widehat{E}^{\mathrm{I}}_{1\parallel}(s) &= -(\gamma + i\omega)\left(\widehat{A}^{\mathrm{R}}_{1\parallel}(s) + i\widehat{A}^{\mathrm{I}}_{1\parallel}(s)\right)
\end{aligned} \tag{5.4}$$

$$\Rightarrow \boxed{\begin{aligned}
\widehat{E}^{\mathrm{R}}_{1\parallel}(s) &= -\gamma\widehat{A}^{\mathrm{R}}_{1\parallel}(s) + \omega\widehat{A}^{\mathrm{I}}_{1\parallel}(s) \\
\widehat{E}^{\mathrm{I}}_{1\parallel}(s) &= -\omega\widehat{A}^{\mathrm{R}}_{1\parallel}(s) - \gamma\widehat{A}^{\mathrm{I}}_{1\parallel}(s)
\end{aligned}}$$

## Simulation Setup

For the plasma beta following values are investigated

$$\beta \in [0.0,\ 0.2,\ 0.4,\ 0.6,\ 0.8,\ 1.0,\ 1.1,\ 1.2,\ 1.4,\ 1.6]\,\% \ . \tag{5.5}$$

The values will be set with the parameter `beta` in the input file. As base input file the cyclone benchmark case provided by the **GKW** Team was used. The input file can be found in the **GKW** repository under `doc/input/cyclone`. Here, the input parameter were adjust for linear $\beta$ scan and are displayed in Table 5.1. Additionally following parameter were set

- `NON_LINEAR` = `.false.` to enable linear simulations,
- `nlepar` = `.true.` to enable the calculatation of $E_{1\parallel}$,
- `io_format` = `'hdf5` output data to `hdf5` format,
- `gama_tol` = $1 \cdot 10^{-5}$ defines tolerance for linear growth rate $\gamma$,
- `adiabatic_electrons` = `.false.` to enable kinetic electrons,
- `mode_box` = `.false.` deactivates 2D mode grid and
- $k_\zeta \rho = 0.3$ defines "poloidal" wave vector which corresponds roughly to the position of the maximum of the nonlinear transport spectrum in **GKW** .

| `DTIM` | `NTIME` | `NAVERAGE` | $N_{\mathrm{mod}}$ | $N_x$ | $N_s$ | $N_{v_\parallel}$ | $N_\mu$ | $N_{\mathrm{sp}}$ | `nperiod` |
|---|---|---|---|---|---|---|---|---|---|
| 0.01 | 2000 | 100 | 1 | 1 | 288 | 64 | 16 | 2 | 5 |

Table 5.1: Adjusted input parameter for linear $\beta$ scan: **Variables**

The simulations were performed local on the maschine `btppx25` and in the University Bayreuth cluster `emil`. Since the simulation perfroms well on the cluster it was shown that parallelization with OpenMPI works. The result of the linear $\beta$ scan can be seen in Figure 5.2. The obtained data shows good agreement with Ref. 17 although due to the different normalization scheme, i.e. GENE normalises with speed of sound and **GKW** normalise by the thermal velocity $v_{\mathrm{th}}$, the values are $\sqrt{2}$ times smaller. Furthermore, one would notice by comparing the beta scan in Ref. 17 and Figure 5.2 that the transition from ion temperature gradient mode (ITG) to trapped electron mode (TEM) and from (TEM) to kinetic balloning mode (KBM) are located at different values of plasma beta $\beta$. This behaviour is due to different values for the wave vector $k_\zeta \rho$ and the resolution of parallel velocity grid $N_{v_\parallel}$.

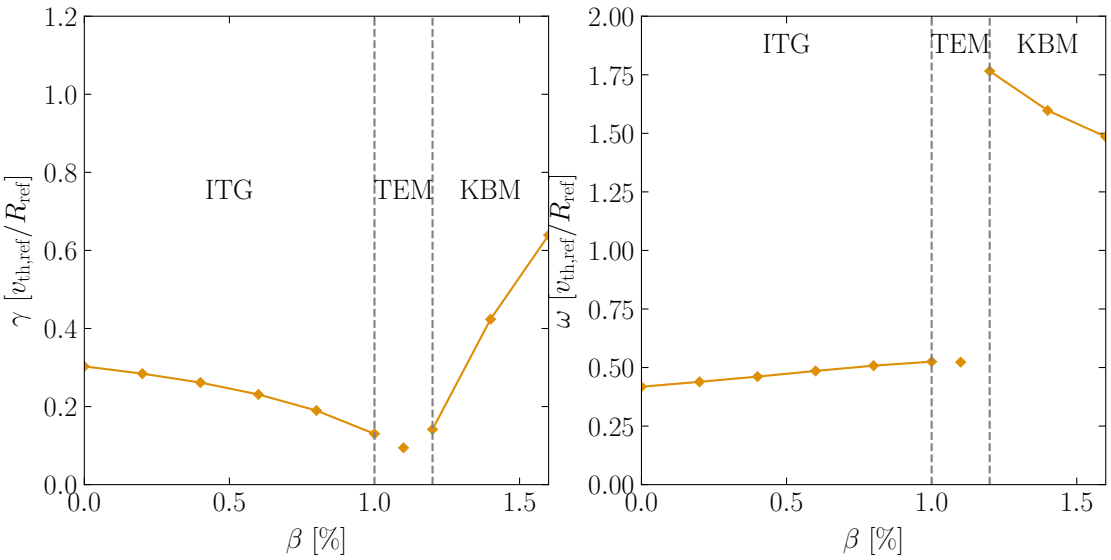


Figure 5.2: Growth rate $\gamma$ and frequency $\omega$ for different plasma beta $\beta$. Here, (ITG) stands for ion temperature gradient modes, (TEM) for trapping electron modes and (KBM) for kinetic balloning modes.

The comparision of the induced electric field $E_{1\parallel}$ and plasma induction $A_{1\parallel}$ yields that the implementation of the $E_{1\parallel}$ field equation was successful. An example of the camparison for $\beta = 0.8\,\%$ is shown in Figure 5.3 and for different plasma beta values in Appendix 7.1.

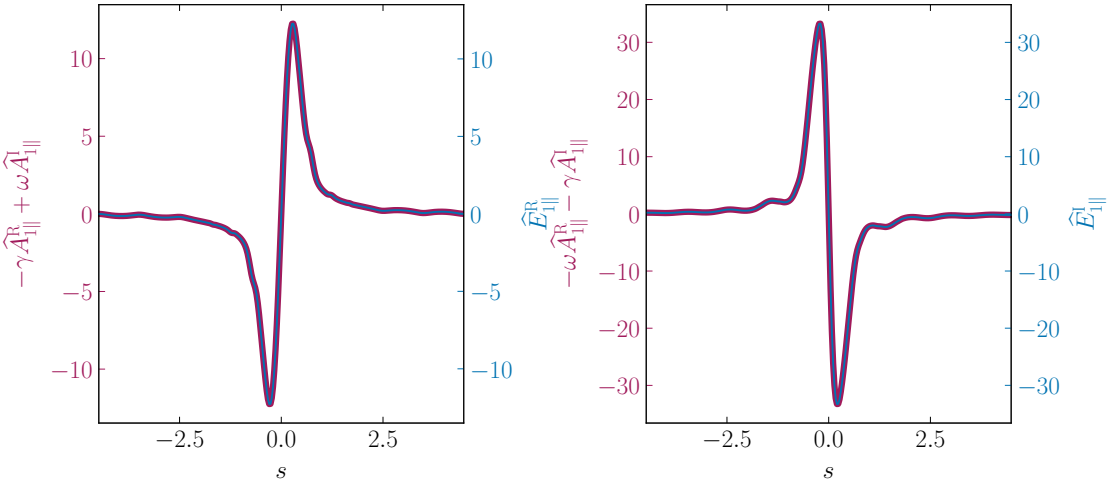


Figure 5.3: Comparision between real and imaginary part of the induced electric field $E_{1\parallel}$ and plasma Induction $A_{1\parallel}$ for $\beta = 0.8\,\%$.

### 5.2.3 $f$ Version of GKW

As stated in Chapter 4.5.4 the current version of **GKW** implements the gyrokinetic equation with the use of the modified distribution function $g$. To preserve the established structure of the code a new numerical scheme gets introduced. To recall the right-hand side of the Vlasov equatiuon $\mathcal{V}$ is definded as

$$\frac{\partial g}{\partial t} = \mathcal{V} \tag{5.6}$$

which is implemented numerical with Runge Kutta (one timestep $(i \to i+1)$) as

$$g^{i+1} = g^i + \Delta t \cdot \left(\mathcal{V}^{i+1}\right) \ . \tag{5.7}$$

To transform the established scheme to the distribution function $F_1$, Equation 4.41 has to be considered and is given by

$$\frac{\partial F_1}{\partial t} = \mathcal{V} + \frac{Zev_\parallel}{T} J_0 E_{1\parallel} F_\mathrm{M} \ , \tag{5.8}$$

where $J_0 E_{1\parallel} = \bar{E}_{1\parallel}$ in the local simulation is and can be written normalised andf fourier transformed as

$$\frac{\partial \widehat{F}_{1\mathrm{N},s}}{\partial t_\mathrm{N}} = \widehat{\mathcal{V}}_\mathrm{N} + \frac{2Zv_\mathrm{thR} v_{\parallel\mathrm{N}}}{T_\mathrm{R}} J_0 \widehat{E}_{1\parallel\mathrm{N}} F_\mathrm{MN} \ . \tag{5.9}$$

Here, the numerical Runge Kutta scheme can be expressed as

$$F_1^{i+1} = F_1^i + \Delta t \cdot \left(\mathcal{V}^{i+1} + \frac{Zev_\parallel}{T} J_0 E_{1\parallel}^{i+1}\right) \ . \tag{5.10}$$

Note that the established numerical scheme using the modified distribution $g$ can easily transform to the scheme using the distribution $F_1$ by appling the so called $E_{1\parallel}$-*Correction* to the RHS. The overall new numerical scheme can be seen in Figure 5.4.

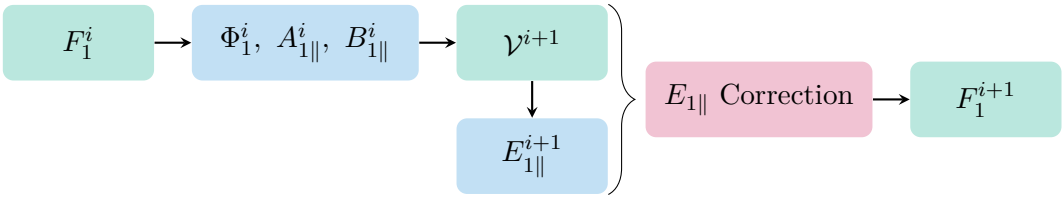


Figure 5.4: Numerical scheme used to calculate the distribution function $F_1$ in **GKW** .

To implement the $E_{1\|}$-Correction a closer look on the already existing $A_{1\|}$-Correction will be made. The $A_{1\|}$-Correction is used to calculate the distrubution $F_1$ from the modified distribution $g$, which is necessary since most of the diagnostics need the distruibution $F_1$ for calculation. To recall $g$ is defined as

$$g = F_1 + \frac{Zev_\|}{T} J_0 A_{1\|} F_\mathrm{M} \ . \tag{5.11}$$

To get the gyrocenter distruibution function $F_1$ one has to subtract the $A_{1\|}$-Term, i.e. the $A_{1\|}$-Correction, from the modified distribution $g$. This gets realised with the use of the matrix `matg2f` which gets definded in the module `matdat`. The elements are set in the subroutine `g2f_correct` in the module `linear_terms` and the calculation for $g$ to $F_1$ gets either performed with a loop over all elements of array `fdisi` or in the function `ge_f_from_g`. Implementing the $E_{1\|}$-Correction follows the same structure. First the matrix `matrhs4f` (RHS for $F_1$) gets introduced in the module `matdat` with `nelem_rhs4f` number of elements defined in the module `dist`. The elements itself are set in the subroutine `epar_correct` the main difference to `g2f_correct` is the swap of minus sign and the use of $E_{1\|}$ instead of $A_{1\|}$. The RHS than gets correct right after the calculation of the $E_{1\|}$ field in the subroutine `calculate_rhs` in the module `exp_integration`. Here, the loop method was used because it was found that the calculation of the new RHS needs 50% longer with the `usmv` subroutine. The code sequence is given below. Note that the $E_{1\|}$-Correction has to be multiplied the time step `deltatime` to have the correct expression for the Runge Kutta scheme.

```
! Apply E|| correction to rhs
! Note that rhs = rhs * dtim so the E|| corrections also has to
! be multipied with dtim
do i = 1, matrhs4f%nmat
  rhs(i) = rhs(i) + deltatime*matrhs4f%mat(i)*fdis(matrhs4f%jj(i))
end do
```

Now that the $E_{1\|}$-Correction is implemented it is important to clearify that the distribution array `fdisi` stores no longer the modified distribution function $g$ instead the gyrocenter distrubution $F_1$. For that purpose from now on if `nlepar` is set to `.true.` **GKW** gets executed in the **f-version**. Otherwise, if `nlepar` is set to `.false.` the so called **g-version** of **GKW** will be used. If `nlepar` is set to `.true.`, **GKW** switches to the f-version of the code. Additionally, a warning messages will be printed, that the user now uses the f-version of **GKW** . If needed, a new switch called `fversion` could be implemented to turn all necessary switches on. Until now `nlepar` will be used for that purpose. In the subroutine `control_initt` one could add additonal switches for the f-version of **GKW** into the given code sequence below.

```
if(lcollisions) then
  l_matcoll = .true.
end if
```

Furthermore, it is necessary to prevent any code sequence which was meant for the modified distrubution function, i.e. the application of the $A_{1\|}$-Correction. For that

any code sequence using the $A_{1\parallel}$-Correction will get deactivated if `nlepar` is set to `.true.`. Since most sequences define a new temporary distribution array `fdis_tmp` and the upcoming code uses this variable it was convienent to just save `fdisi` in `fdis_tmp` for the f-version of **GKW** . Additionally, the function `get_f_from_g` gets modified to return just `fdisi` and the definition of the matrix `matg2f` gets supressed as well to save disk space during execution.

As last step the field equation of the perturbated vector potential $A_{1\parallel}$ has to be adjusted, since it is the only field equation which changes significantly through the substitution of the modified distribution $g$ [Ch. 4.5.4]. For that, an if statemant for the f-version gets introduced intoe the subroutine `ampere_dia` in the module `linear_terms` which deactivates the skin term if `nlepar` is set to `.true.`. As already mentioned the other field equation are still implemented right for `fdisi` as distribution $F_1$.

### Benchmark of $f$ Version of GKW - Linear $\beta$ Scan

### 5.2.4 Nonlinear Terms

Until now only the linear terms of the gyrokinetic equations got discussed. To complete the transformation to the f-version **GKW** the nonlinear terms has to be considered as well. Because of the substitition of the modified distribution function $g$ the nonlinear terms

$$\mathbf{v}_\chi \cdot \nabla F_1 \;\&\; -\frac{F_\mathrm{M}}{T}\mathbf{v}_{\bar{B}_{1\perp}} \cdot (Ze\nabla\bar{\Phi} + \mu\nabla\bar{B}_{1\parallel})$$

got replaced with $\mathbf{v}_\chi \cdot \nabla g$. To implement the nonlinear terms one has simple to insert the definition of the modified distribution into the already implemented nonlinear term. This results in the following relation

$$\begin{aligned}
\mathbf{v}_\chi \cdot \nabla g &= \mathbf{v}_\chi \cdot \nabla \left( F_1 + \frac{Zev_\parallel}{T}\bar{A}_{1\parallel}F_\mathrm{M} \right) \\
&= \mathbf{v}_\chi \cdot \nabla F_1 + \mathbf{v}_\chi \cdot \nabla \left( \frac{Zev_\parallel}{T}\bar{A}_{1\parallel}F_\mathrm{M} \right) \\
&= \mathbf{v}_\chi \cdot \nabla F_1 + \frac{ZeF_\mathrm{M}}{T}\mathbf{v}_\chi \cdot \nabla(v_\parallel \bar{A}_{1\parallel}) \\
&= \mathbf{v}_\chi \cdot \nabla F_1 + \frac{ZeF_\mathrm{M}}{T}\mathbf{v}_{\bar{B}_{1\perp}} \cdot \left( \nabla\bar{\Phi} - \nabla(v_\parallel \bar{A}_{1\parallel}) + \frac{\mu}{Ze}\nabla\bar{B}_{1\parallel} \right) \\
&= \mathbf{v}_\chi \cdot \nabla F_1 + \frac{F_\mathrm{M}}{T}\mathbf{v}_{\bar{B}_{1\perp}} \cdot (Ze\nabla\bar{\Phi} + \mu\nabla\bar{B}_{1\parallel}) \;,
\end{aligned} \tag{5.12}$$

although the term with $\mathbf{v}_\chi \cdot \nabla F_\mathrm{M}$ gets neglected due to order of $\rho_\star^2$. Since the introduction of the f-version of **GKW** the distribution array `fdisi` is already $F_1$, so only the $A_{1\parallel}$ term has to be added to `fdisi`, i.e. apply the $A_{1\parallel}$ correction. For that a new matrix `matf2g` gets introduced which basically is the same as `matg2f` only the minus signs of the elements are swap. For convienence, the elements for `matf2g` will be set in subroutine `apar_correct`. The $A_{1\parallel}$ correction itself gets performed via loop over the elements of `fdisi` in the subroutine `add_non_linear_terms` and saved in the temporary distribution array `fdis_tmp`. Then, the array `fdis_tmp` will be used to calculate the nonlinear terms. It is important to insure the usage of `fdis_tmp` only since in the f-version the distribution $F_1$ gets used for further calculation and should not be changed. To advance errors `fdis_tmp` will be written as well, if the f-version is not used and is simply the array `fdisi`. The above implementation is valid if `nlepar` and `non_linear` is set to `.true.`.

CHAPTER

# 6

# Conclusion

In this thesis the minimal resolution for simulations with **GKW** in the Cyclone Base parameter were observed in which the number of grid points for the parallel velocity $N_{v_\parallel}$ could be reduced from 64 to 48, which halfed the time until suppression of turbulence.

Additionally, the active development of a restart script in `python3` led to further convenience during the task of performing simulations on the `btrzx1` cluster.

Through careful tests this bachelor thesis confirms the radial size convergence of the $\mathrm{E} \times \mathrm{B}$ staircase pattern in local gyrokinetic flux tube simulations of ion temperature gradient (ITG)-driven turbulence. A mesoscale pattern size of $\sim 57 - 76\,\rho_{\mathrm{th}}$ is found to be intrinsic to ITG-driven turbulence for Cyclone Base Case parameters. This length scale is somewhat larger compared to results from global studies with finite $\rho_*$, which report of a few $10\,\rho_{\mathrm{th}}$**?** , and has to be considered the proper mesoscale in the local limit $\rho_* \to 0$. The occurrence of this mesoscale implies that non-locality, in terms of Ref. **?** , is inherent to ITG-driven turbulence, since avalanches are spatially organized by the $\mathrm{E} \times \mathrm{B}$ staircase pattern**? ?** [18]**?** .

CHAPTER

# 7

# Appendix

## 7.1 Comparision between $E_{1\parallel}$ and $A_{1\parallel}$ for various plasma beta

### For the g-version of GKW

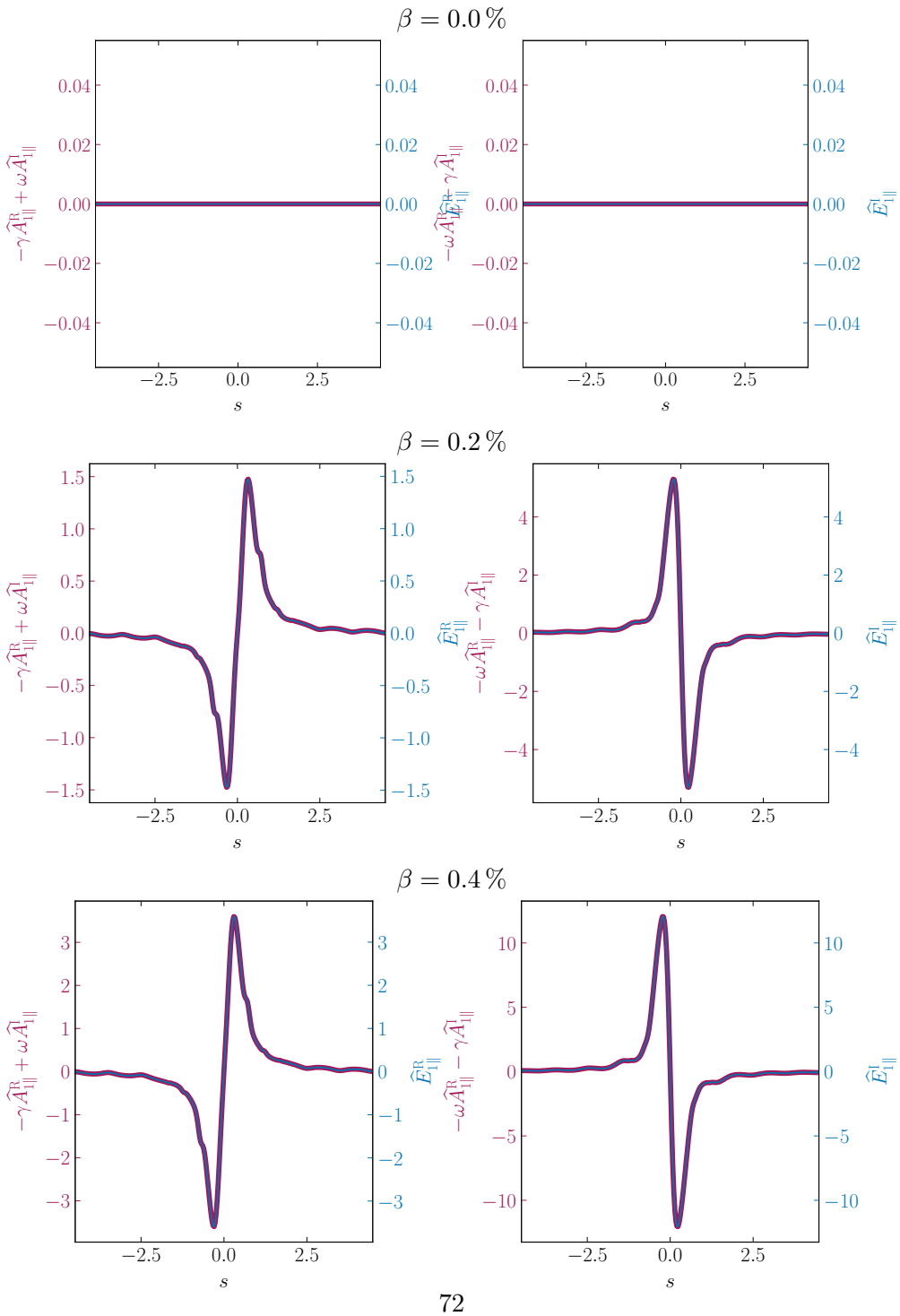

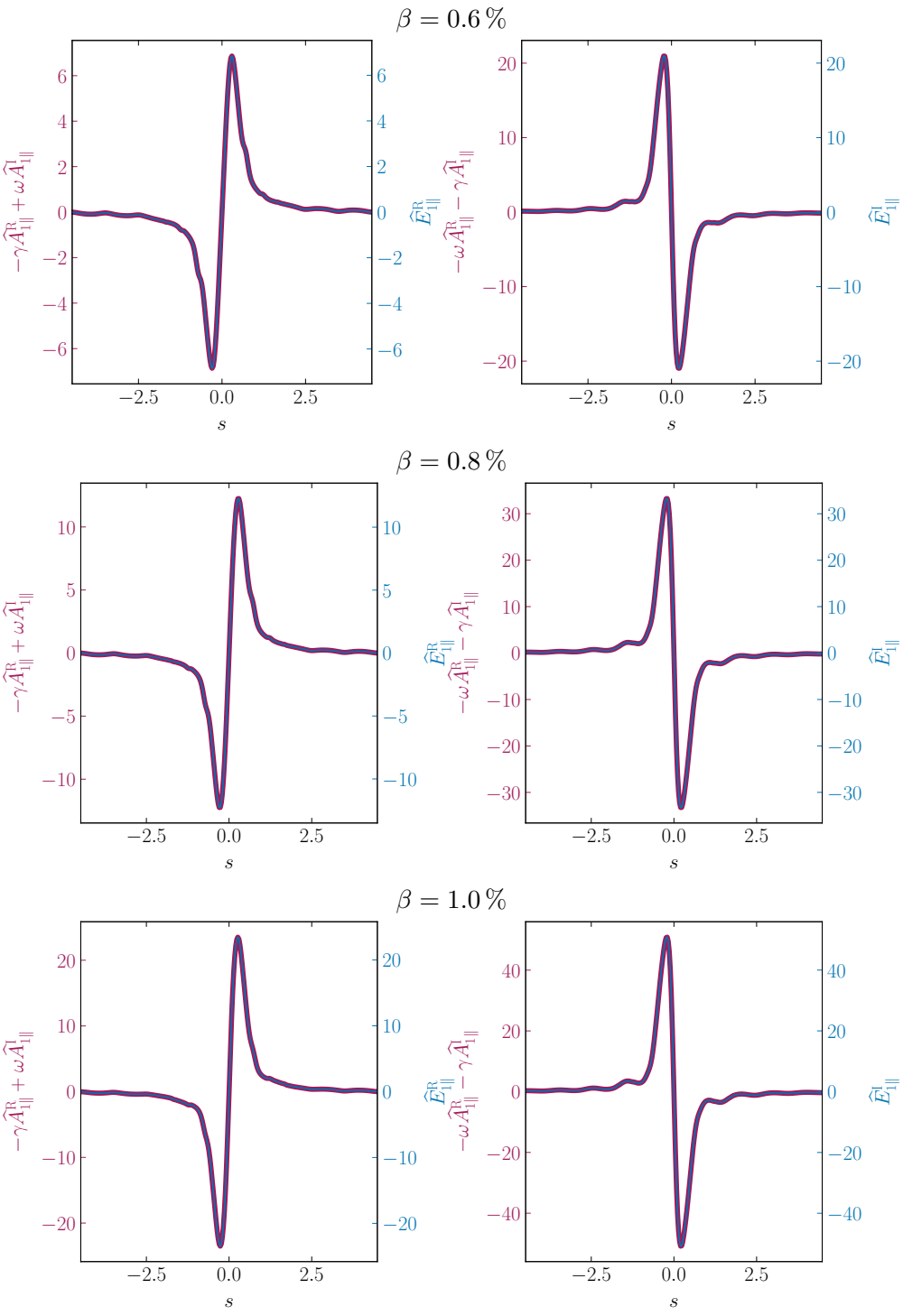
$\beta = 0.6\,\%$
$\beta = 0.8\,\%$
$\beta = 1.0\,\%$
$-\gamma\widehat{A}^{\mathrm{R}}_{1\|} + \omega\widehat{A}^{\mathrm{I}}_{1\|}$
$\widehat{E}^{\mathrm{R}}_{1\|}$
$-\omega\widehat{A}^{\mathrm{R}}_{1\|} - \gamma\widehat{A}^{\mathrm{I}}_{1\|}$
$\widehat{E}^{\mathrm{I}}_{1\|}$
$s$

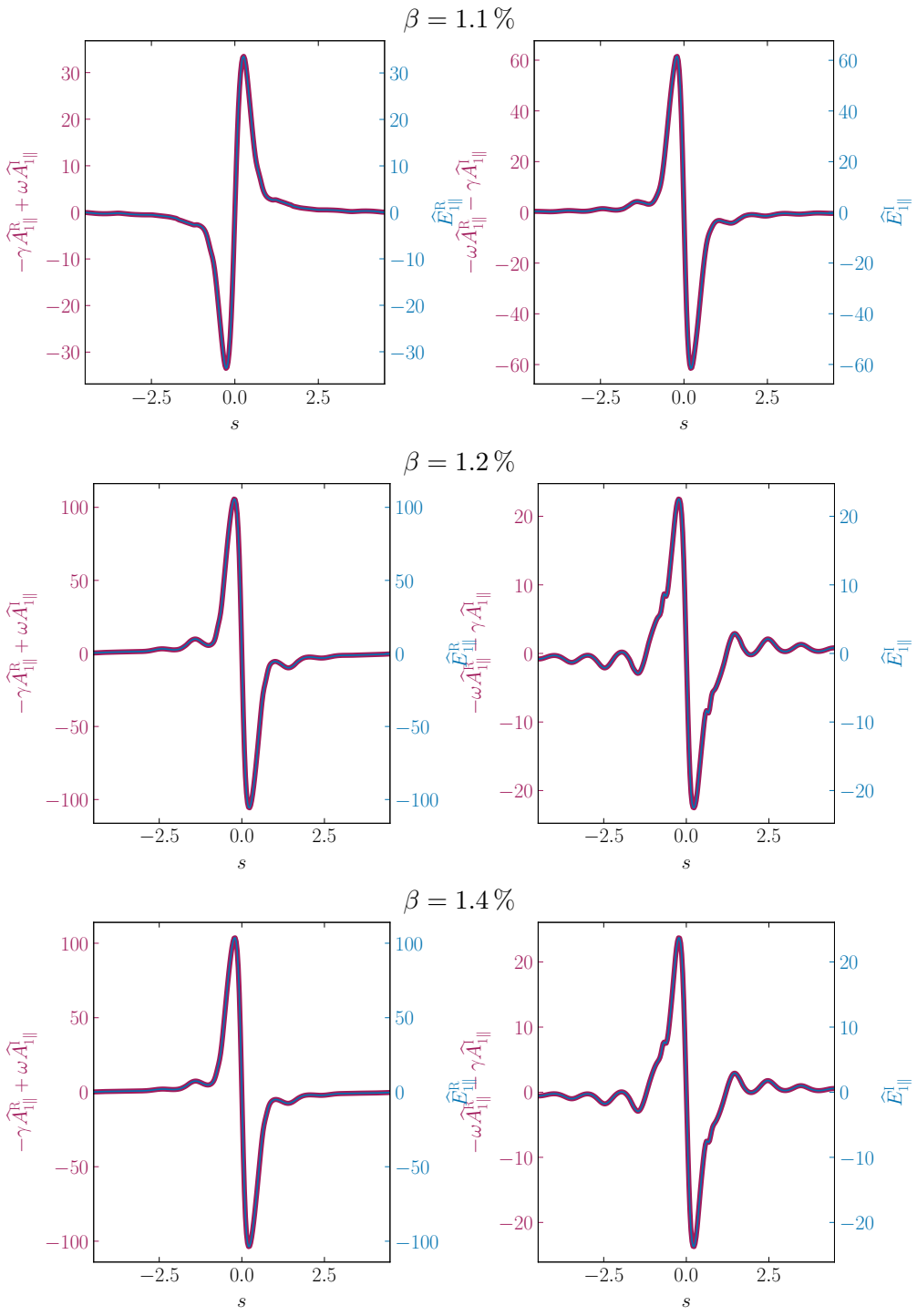
$\beta = 1.1\,\%$
$-\gamma\widehat{A}^{\mathrm{R}}_{1\parallel} + \omega\widehat{A}^{\mathrm{I}}_{1\parallel}$
$\widehat{E}^{\mathrm{R}}_{1\parallel}$
$-\omega\widehat{A}^{\mathrm{R}}_{1\parallel} - \gamma\widehat{A}^{\mathrm{I}}_{1\parallel}$
$\widehat{E}^{\mathrm{I}}_{1\parallel}$
$s$
$\beta = 1.2\,\%$
$-\gamma\widehat{A}^{\mathrm{R}}_{1\parallel} + \omega\widehat{A}^{\mathrm{I}}_{1\parallel}$
$\widehat{E}^{\mathrm{R}}_{1\parallel}$
$-\omega\widehat{A}^{\mathrm{R}}_{1\parallel} - \gamma\widehat{A}^{\mathrm{I}}_{1\parallel}$
$\widehat{E}^{\mathrm{I}}_{1\parallel}$
$s$
$\beta = 1.4\,\%$
$-\gamma\widehat{A}^{\mathrm{R}}_{1\parallel} + \omega\widehat{A}^{\mathrm{I}}_{1\parallel}$
$\widehat{E}^{\mathrm{R}}_{1\parallel}$
$-\omega\widehat{A}^{\mathrm{R}}_{1\parallel} - \gamma\widehat{A}^{\mathrm{I}}_{1\parallel}$
$\widehat{E}^{\mathrm{I}}_{1\parallel}$
$s$

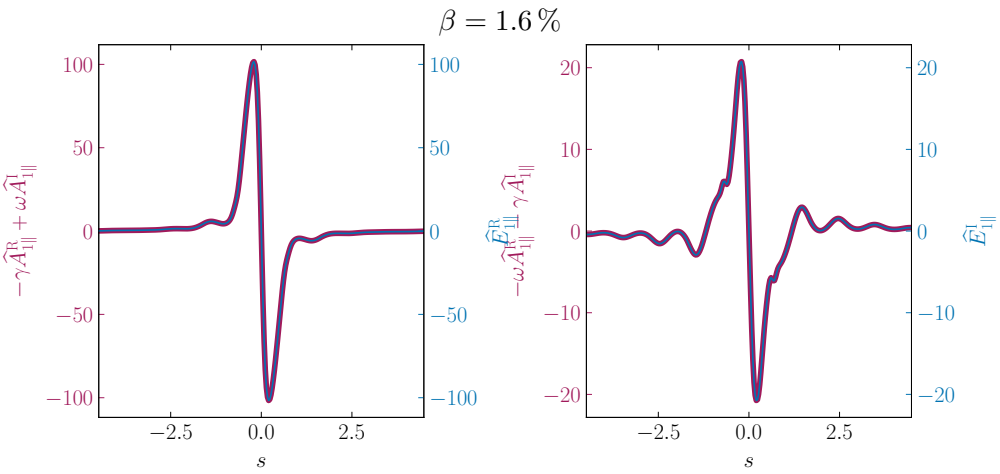
$\beta = 1.6\,\%$
$-\gamma \widehat{A}^{\mathrm{R}}_{1\|} + \omega \widehat{A}^{\mathrm{I}}_{1\|}$
$-\omega \widehat{A}^{\mathrm{R}}_{1\|} - \gamma \widehat{A}^{\mathrm{I}}_{1\|}$
$\widehat{E}^{\mathrm{R}}_{1\|}$
$\widehat{E}^{\mathrm{I}}_{1\|}$
$s$
$s$

**For the f-version of GKW**

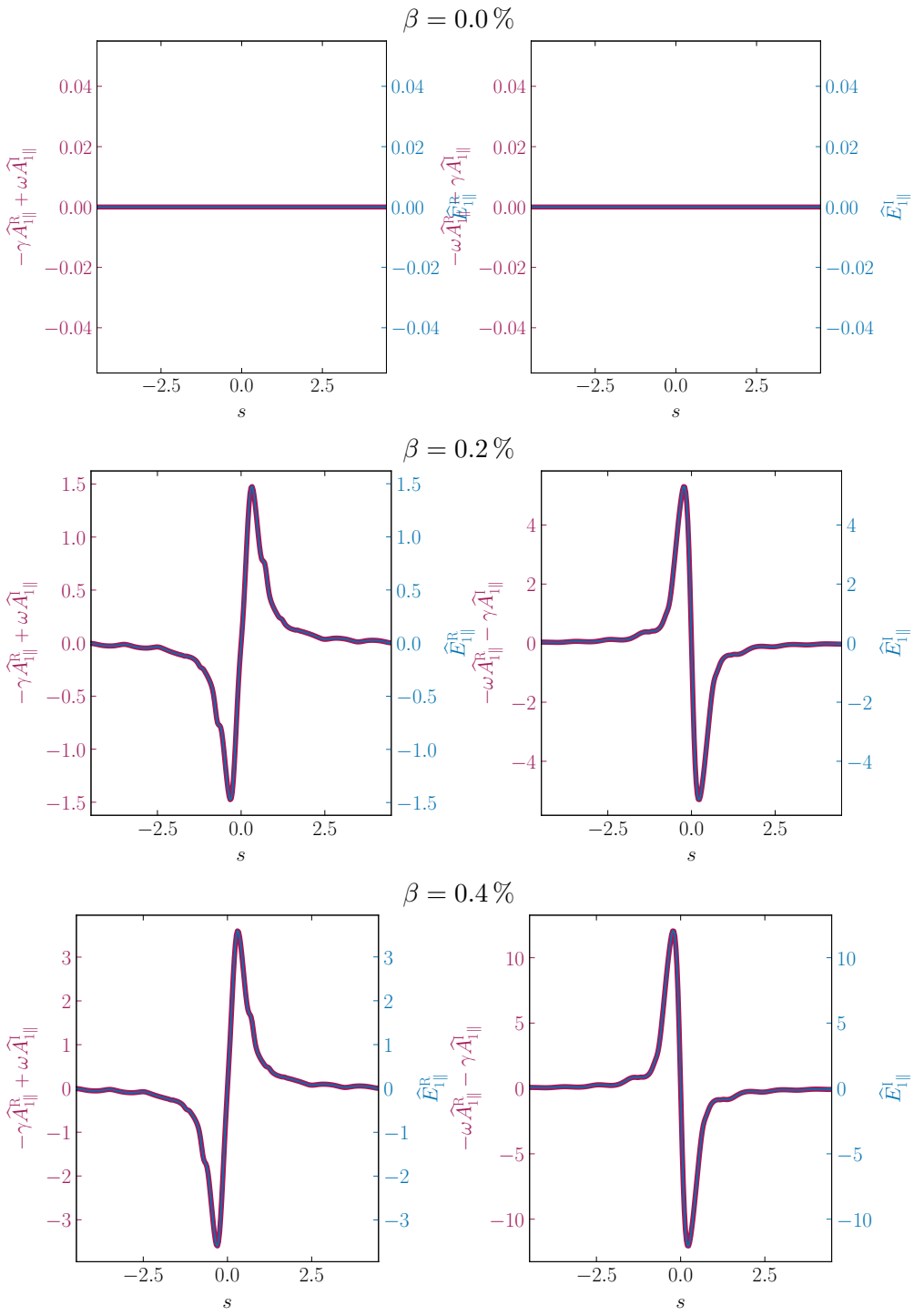

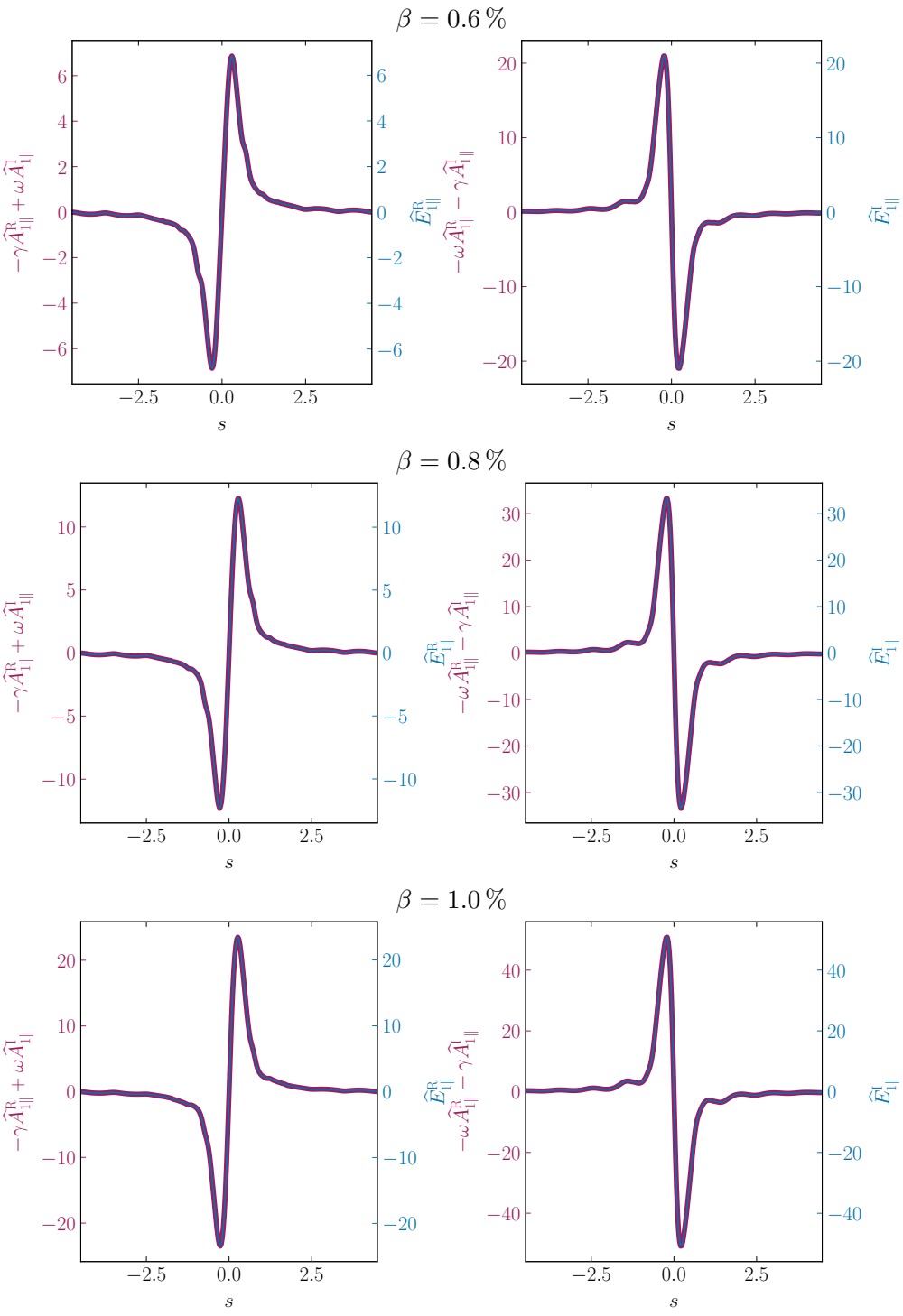
$\beta = 0.6\,\%$
$\beta = 0.8\,\%$
$\beta = 1.0\,\%$
$-\gamma \widehat{A}^{\mathrm{R}}_{1\parallel} + \omega \widehat{A}^{\mathrm{I}}_{1\parallel}$
$\widehat{E}^{\mathrm{R}}_{1\parallel}$
$-\omega \widehat{A}^{\mathrm{R}}_{1\parallel} - \gamma \widehat{A}^{\mathrm{I}}_{1\parallel}$
$\widehat{E}^{\mathrm{I}}_{1\parallel}$
$s$

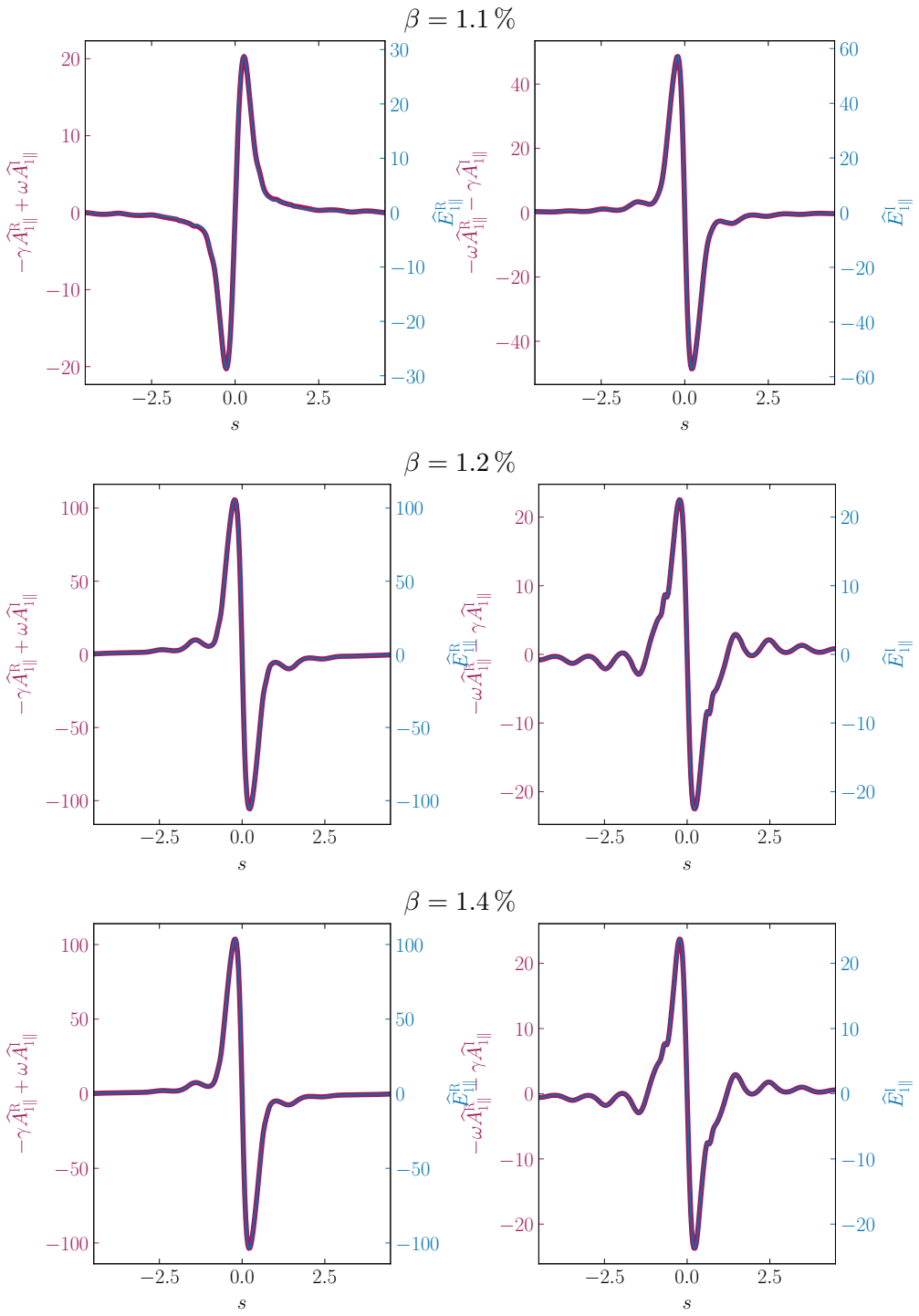
$\beta = 1.1\,\%$
$-\gamma\widehat{A}^{\mathrm{R}}_{1\parallel} + \omega\widehat{A}^{\mathrm{I}}_{1\parallel}$
$-\omega\widehat{A}^{\mathrm{R}}_{1\parallel} - \gamma\widehat{A}^{\mathrm{I}}_{1\parallel}$
$\widehat{E}^{\mathrm{I}}_{1\parallel}$
$s$
$\beta = 1.2\,\%$
$-\gamma\widehat{A}^{\mathrm{R}}_{1\parallel} + \omega\widehat{A}^{\mathrm{I}}_{1\parallel}$
$-\omega\widehat{A}^{\mathrm{R}}_{1\parallel} - \gamma\widehat{A}^{\mathrm{I}}_{1\parallel}$
$\widehat{E}^{\mathrm{I}}_{1\parallel}$
$s$
$\beta = 1.4\,\%$
$-\gamma\widehat{A}^{\mathrm{R}}_{1\parallel} + \omega\widehat{A}^{\mathrm{I}}_{1\parallel}$
$-\omega\widehat{A}^{\mathrm{R}}_{1\parallel} - \gamma\widehat{A}^{\mathrm{I}}_{1\parallel}$
$\widehat{E}^{\mathrm{I}}_{1\parallel}$
$s$

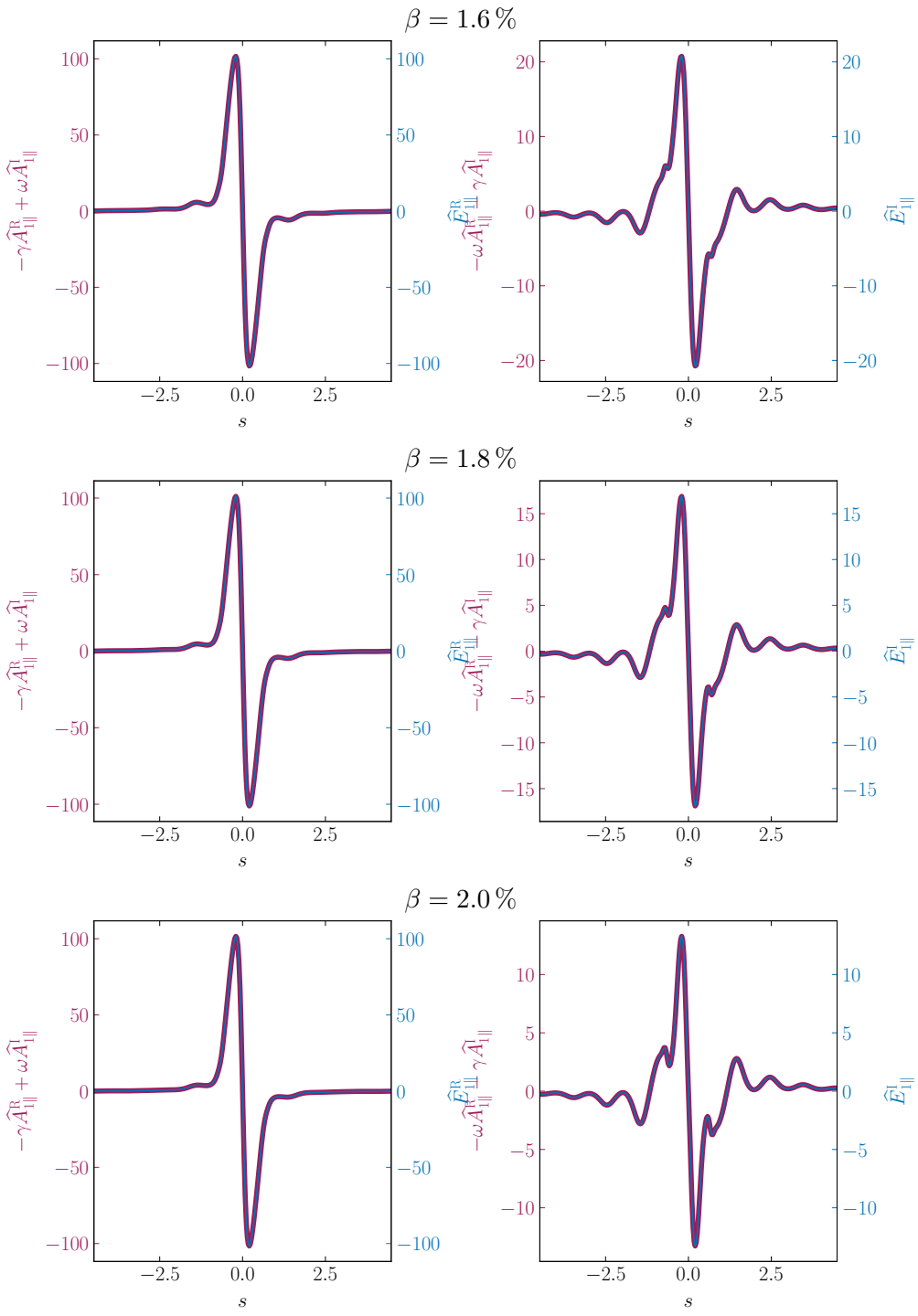
$\beta = 1.6\,\%$
$\beta = 1.8\,\%$
$\beta = 2.0\,\%$
$-\gamma\widehat{A}^{\mathrm{R}}_{1\|} + \omega\widehat{A}^{\mathrm{I}}_{1\|}$
$-\omega\widehat{A}^{\mathrm{R}}_{1\|} - \gamma\widehat{A}^{\mathrm{I}}_{1\|}$
$\widehat{E}^{\mathrm{I}}_{1\|}$
$s$

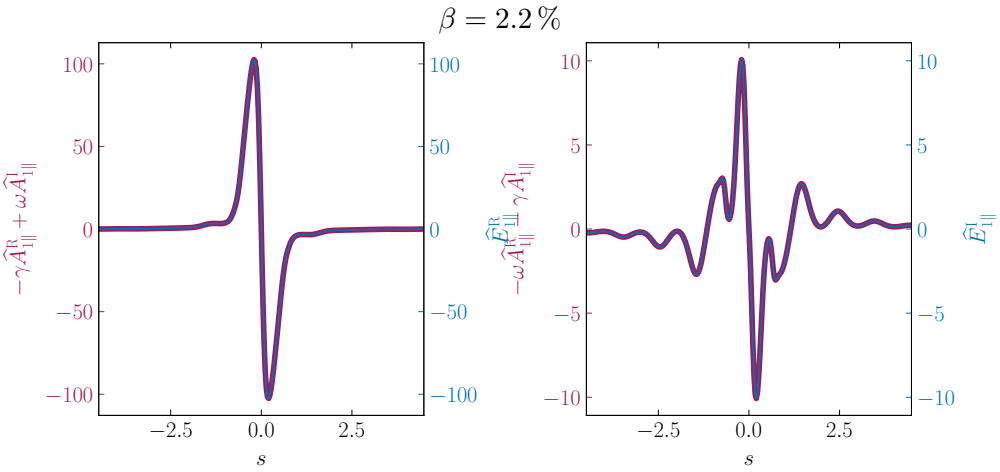
$\beta = 2.2\,\%$
$-\gamma \widehat{A}^{\mathrm{R}}_{1\|\|} + \omega \widehat{A}^{\mathrm{I}}_{1\|\|}$
$-\omega \widehat{A}^{\mathrm{R}}_{1\|\|} - \gamma \widehat{A}^{\mathrm{I}}_{1\|\|}$
$\widehat{E}^{\mathrm{R}}_{1\|\|}$
$\widehat{E}^{\mathrm{I}}_{1\|\|}$
$s$
$s$

CHAPTER

# 8

# Bibliography


[1] Barton, Justin E., Wehner, William P., Schuster, Eugenio, Felici, Federico & Sauter, Olivier 2015 Simultaneous closed-loop control of the current profile and the electron temperature profile in the TCV tokamak. In *2015 American Control Conference (ACC)*, pp. 3316–3321. Chicago, IL, USA: IEEE.

[2] Brizard, A. J. & Hahm, T. S. 2007 Foundations of nonlinear gyrokinetic theory. *Reviews of Modern Physics* **79** (2), 421–468.

[3] Chen, Yang & Parker, Scott 2001 Gyrokinetic turbulence simulations with kinetic electrons. *Physics of Plasmas* **8** (5), 2095–2100.

[4] Crandall, Paul Charles 2019 *Collisional and Electromagnetic Physics in Gyrokinetic Models*. PhD thesis.

[5] Cummings, J. C. 1995 *Gyrokinetic Simulation of Finite-Beta and Self-Generated Sheared-Flow Effects on Pressure-Gradient-Driven Instabilities*. PhD thesis, Princeton University.

[6] Dannert, Tilman 2004 *Gyrokinetische Simulation von Plasmaturbulenz mit gefangenen Teilchen und elektromagnetischen Effekten*. PhD thesis.

[7] Garbet, X., Idomura, Y., Villard, L. & Watanabe, T.H. 2010 Gyrokinetic simulations of turbulent transport. *Nuclear Fusion* **50** (4), 043002.

[8] Krommes, John A. & Kim, Chang-Bae 2000 Interactions of disparate scales in drift-wave turbulence. *Physical Review E* **62** (6), 8508–8539.

[9] Lippert, M. 2024 GKW Branch feature/feature_Epar_extension. https://bitbucket.org/gkw/gkw/branch/feature/feature_Epar_extension.

[10] Maurer, Maurice 2020 *GENE-3D - a Global Gyrokinetic Turbulence Code for Stellarators and Perturbed Tokamaks*. PhD thesis.

[11] Merlo, Gabriele 2016 *Flux-Tube and Global Grid-Based Gyrokinetic Simulations of Plasma Microturbulence and Comparisons with Experimental TCV Measurements*. PhD thesis.

[12] Mishchenko, Alexey, Bottino, Alberto, Hatzky, Roman, Sonnendrücker, Eric, Kleiber, Ralf & Könies, Axel 2017 Mitigation of the cancellation problem in the gyrokinetic particle-in-cell simulations of global electromagnetic modes. *Physics of Plasmas* **24** (8), 081206.

[13] Naitou, Hiroshi, Tsuda, Kenji, Lee, W W & Sydora, R D 1995 Gyrokinetic simulation of internal kink modes .

[14] Peeters, A.G., Camenen, Y., Casson, F.J., Hornsby, W.A., Snodin, A.P., Strintzi, D. & Szepesi, G. 2009 The nonlinear gyro-kinetic flux tube code GKW. *Computer Physics Communications* **180** (12), 2650–2672.

[15] Peeters, A. G., Buchholz, R., Camenen, Y., Casson, F. J., Grosshauser, S. R., Hornsby, W. A., Manas, P., Migliano, P., Siccinio, M., Snodin, A. P., Strintzi, D., Sung, T., Szepesi, G. & Zarzoso, D. 2016 GKW how and why.

[16] Peeters, A. G., Strintzi, D., Camenen, Y., Angioni, C., Casson, F. J., Hornsby, W. A. & Snodin, A. P. 2009 Influence of the centrifugal force and parallel dynamics on the toroidal momentum transport due to small scale turbulence in a tokamak. *Physics of Plasmas* **16** (4), 042310.

[17] Pueschel, M. J., Kammerer, M. & Jenko, F. 2008 Gyrokinetic turbulence simulations at high plasma beta. *Physics of Plasmas* **15** (10), 102310.

[18] Rath, F., Peeters, A. G., Buchholz, R., Grosshauser, S. R., Migliano, P., Weikl, A. & Strintzi, D. 2016 Comparison of gradient and flux driven gyro-kinetic turbulent transport. *Physics of Plasmas* **23** (5), 052309.

[19] Stroth, Ulrich 2018 *Plasmaphysik: Phänomene, Grundlagen und Anwendungen*. Berlin, Heidelberg: Springer Berlin Heidelberg.

[20] Szepesi, G. 2023 Derivation of the fully electro-magnetic, non-linear, gyrokinetic Vlasov–Maxwell equations in a rotating frame of reference for GKW with Lie transform perturbation method .

[21] Told, D. 2012 *Fluctuations of the Electron Temperature Due to Plasma Turbulence in an Internal Transport Barrier Discharge of the TCV Tokamak.*. PhD thesis, University Ulm.

[22] Wesson, J. 2004 *Tokamaks*, 3. Oxford University Press.

# Eidesstattliche Erklärung

Hiermit erkläre ich, Manuel Lippert, dass ich die vorliegende Arbeit selbständig und ohne Benutzung anderer als der angegebenen Hilfsmittel angefertigt habe. Alle Stellen,

die wörtlich oder sinngemäß aus veröffentlichten oder nicht veröffentlichten Schriften entnommen wurden, sind als solche kenntlich gemacht. Die Arbeit hat in gleicher oder

ähnlicher Form noch keiner anderen Prüfungsbehörde vorgelegen.

Bayreuth, den 30.06.2023

_____

Manuel Lippert